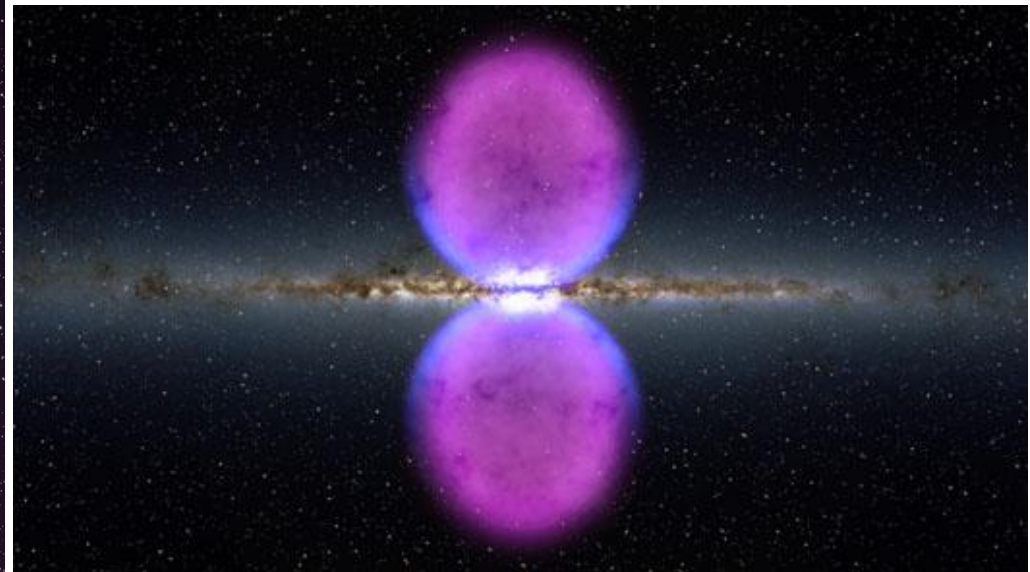


Extended Lobes in AGN at High Energies

Lukasz Stawarz

ISAS/JAXA (Japan)

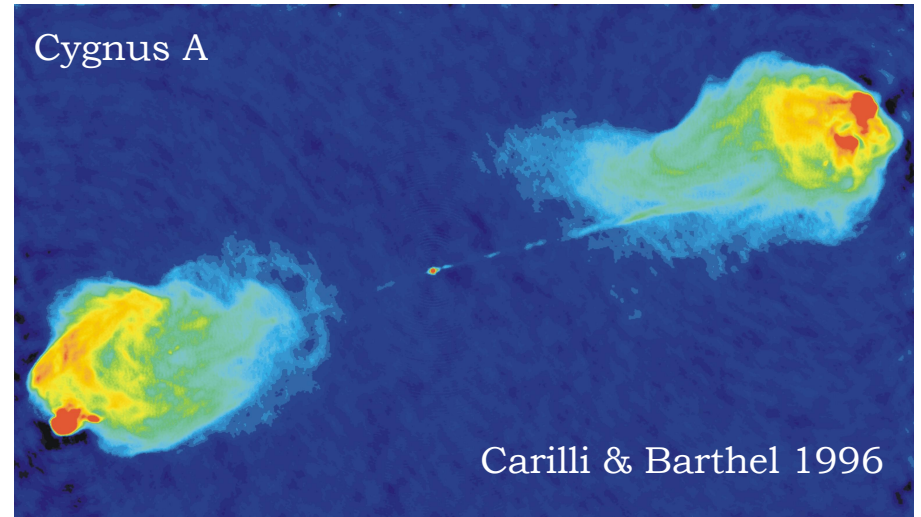
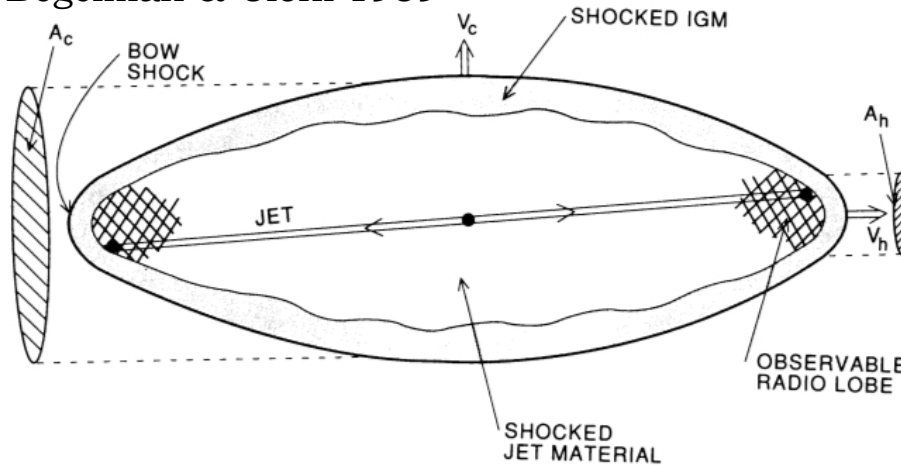
Jagiellonian University (Poland)



***“The Fermi Bubbles:
Theory and Observations”***
SLAC National Accelerator Laboratory
Menlo Park CA (April 11 - 12, 2013)

Classical Doubles

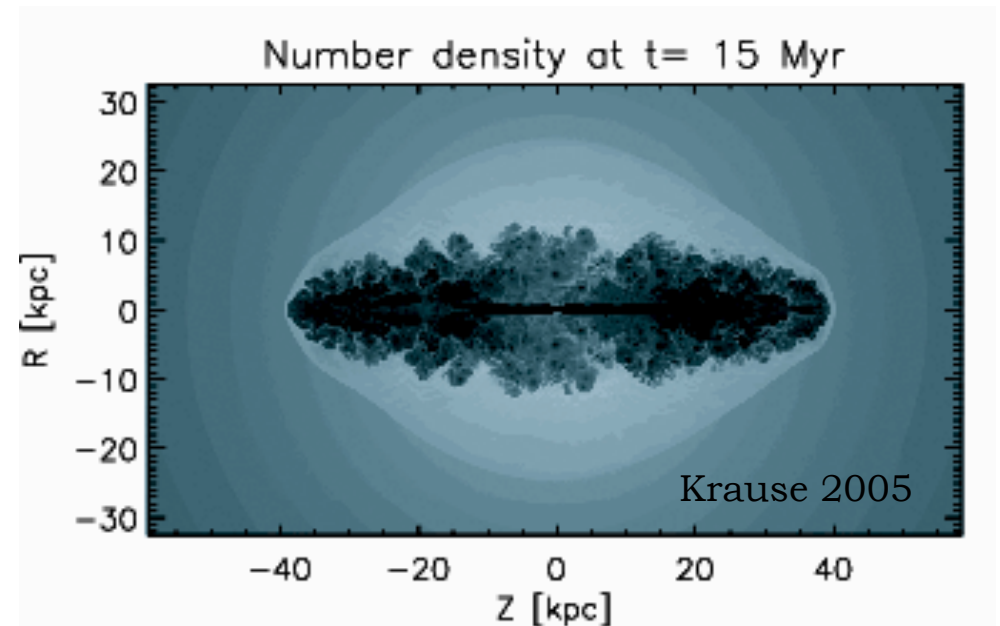
Begelman & Cioffi 1989



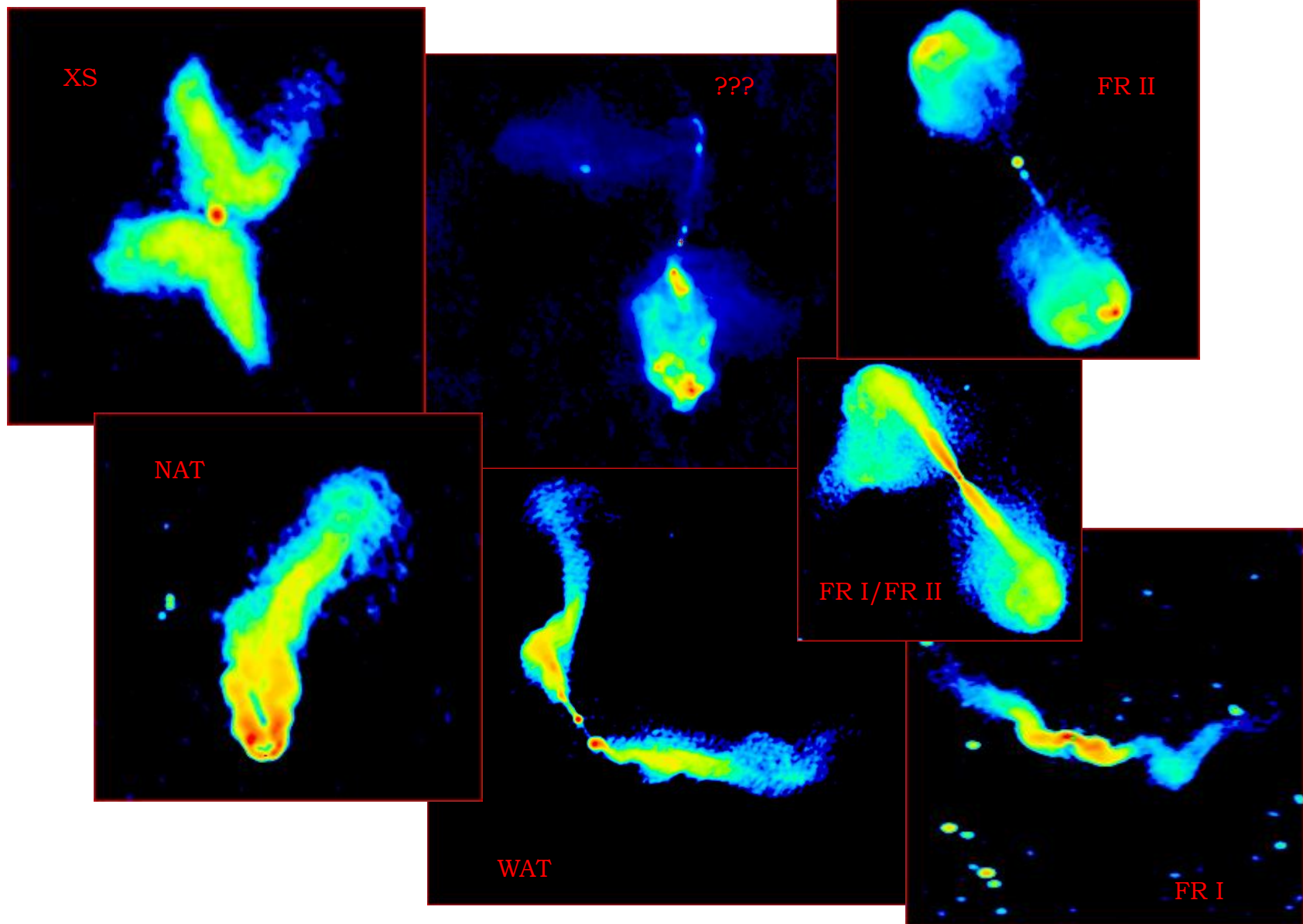
Blandford & Rees 1974, Scheuer 1974:

- Relativistic jets inflate a cavity which expands in a hot gaseous medium
- Extended lobes contain exclusively ultrarelativistic magnetized plasma deposited by relativistic outflows
- Lobes are over-pressured/in pressure equilibrium with the ambient medium

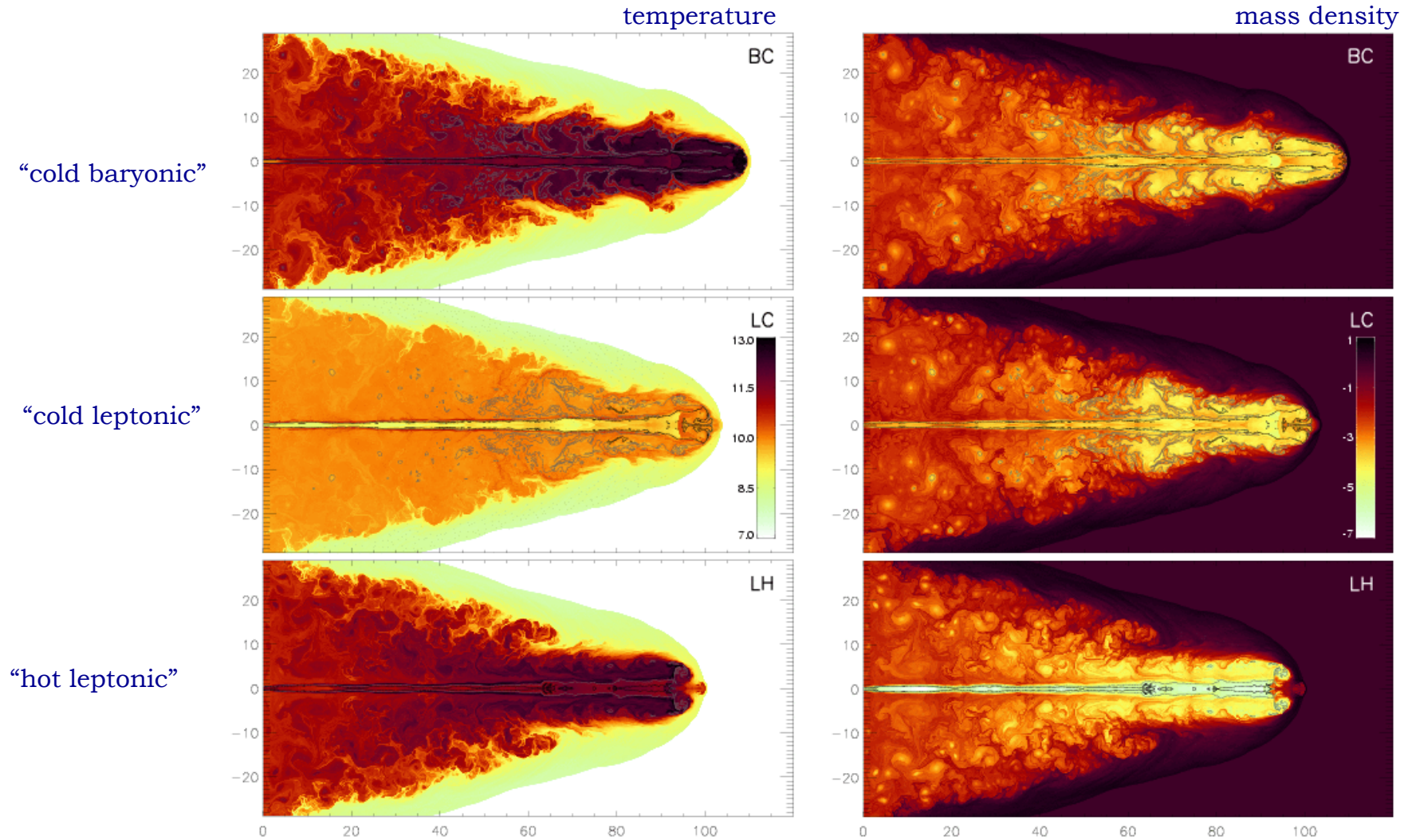
$$\begin{aligned} \rho_{\text{lobe}} &< \rho_{\text{jet}} < \rho_{\text{igm}} \\ P_{\text{lobe}} &> p_{\text{jet}} \geq p_{\text{igm}} \\ n_e/n_p &= ? \\ U_e/U_B &= ? \\ n_{\text{gas}}, T_{\text{gas}} &= ? \end{aligned}$$



Diverse Morphologies



Leptonic or Hadronic?

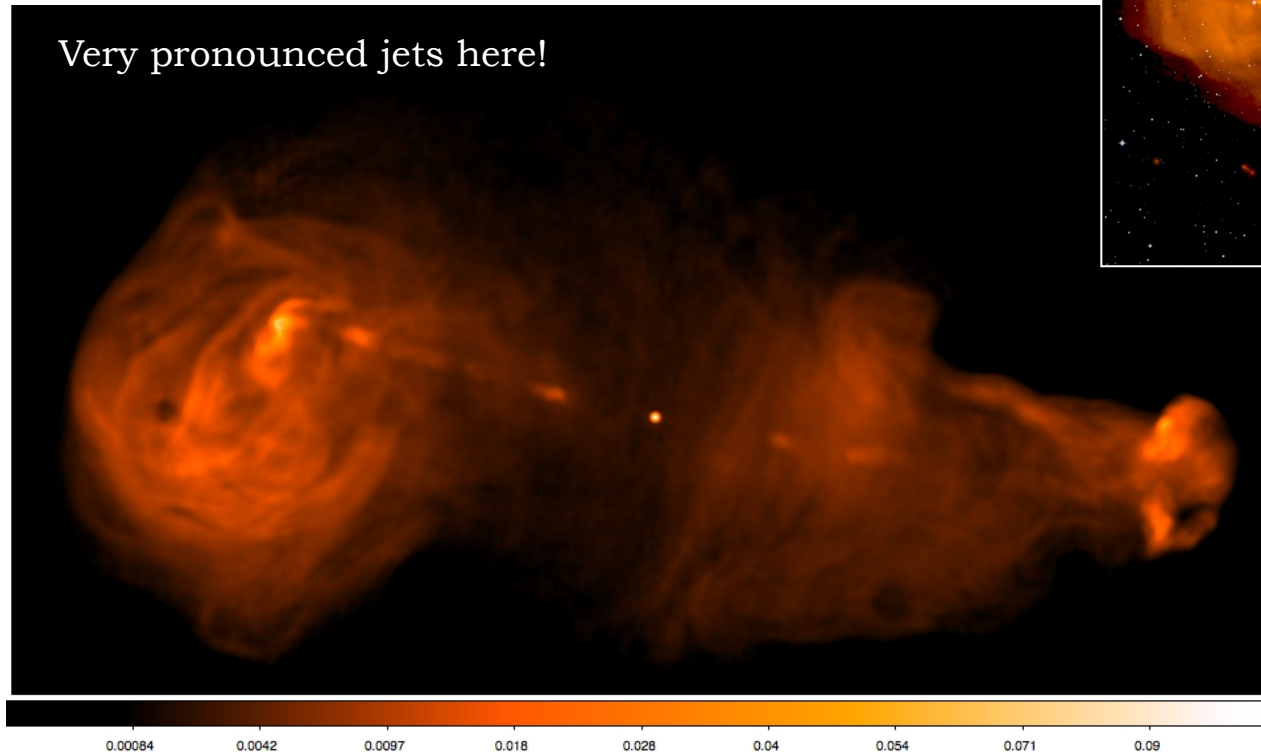
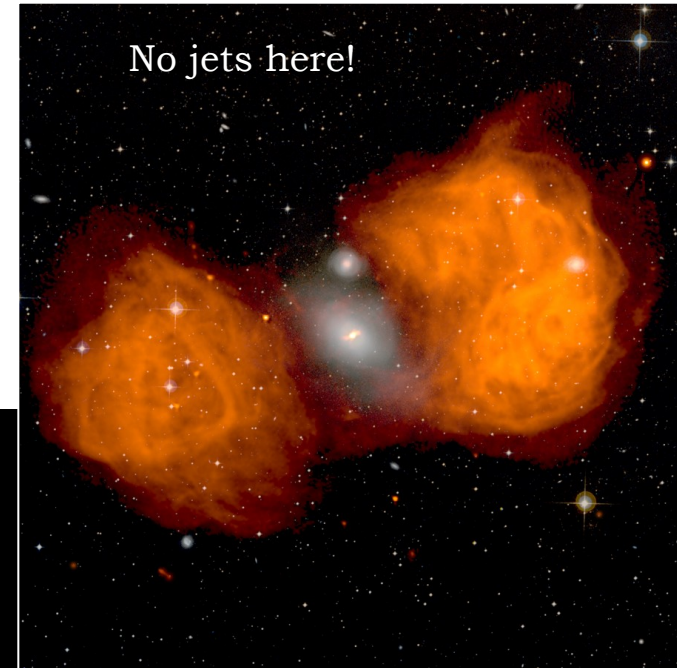


Relativistic jets with the hadronic ($p+e^-$) or purely leptonic (e^+e^-) content produce similar lobes (Scheck et al. 2002)

What About Magnetic Field?

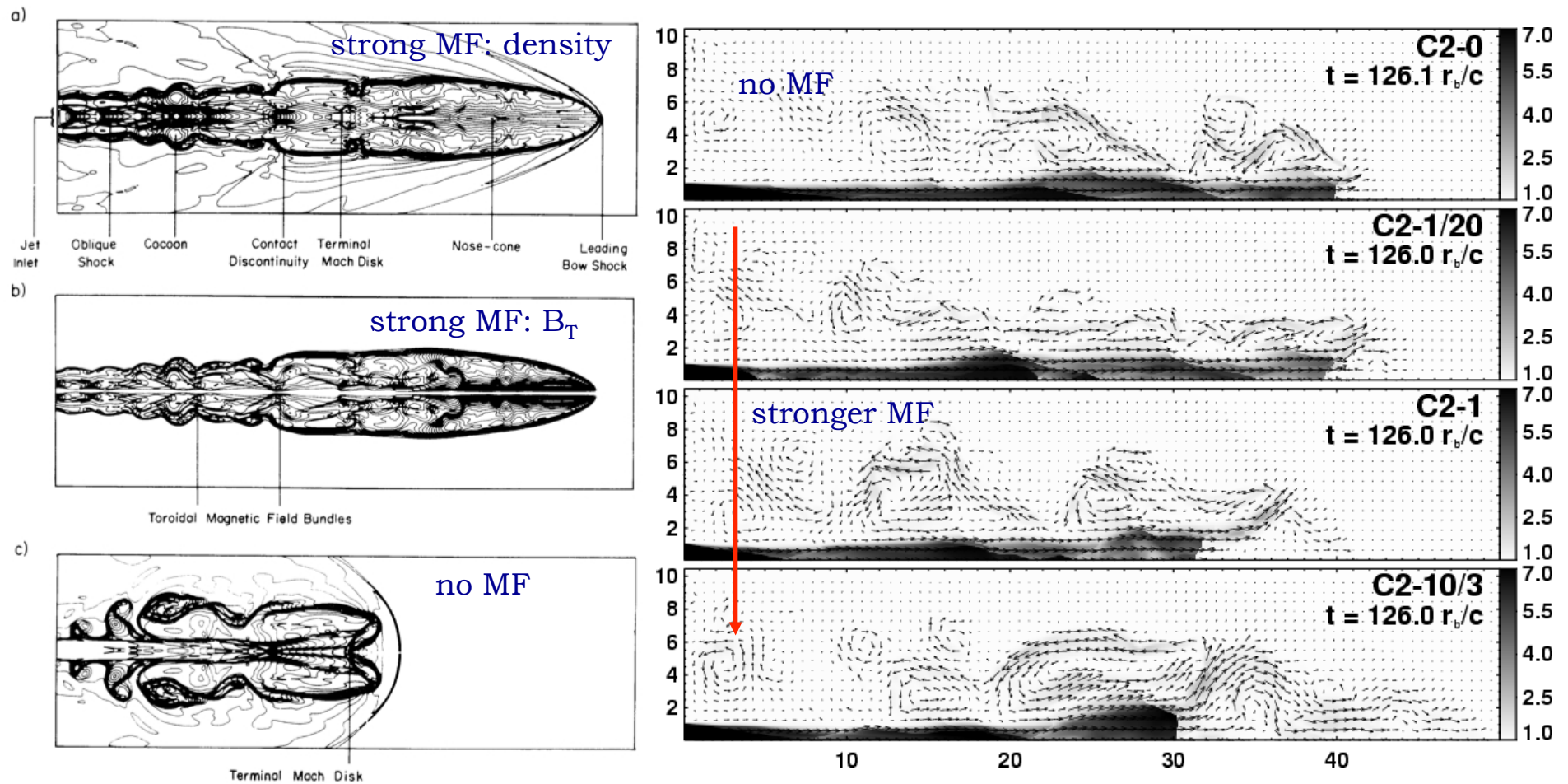
Polarized, power-law synchrotron continuum with spectral indices $0.5 \leq \alpha \leq 1$ within the observable range 10 MHz - 100 GHz (meaning >GeV energy electrons).

“even dynamically subdominant, magnetic field can have crucial effects on lobes’ evolution and stability”



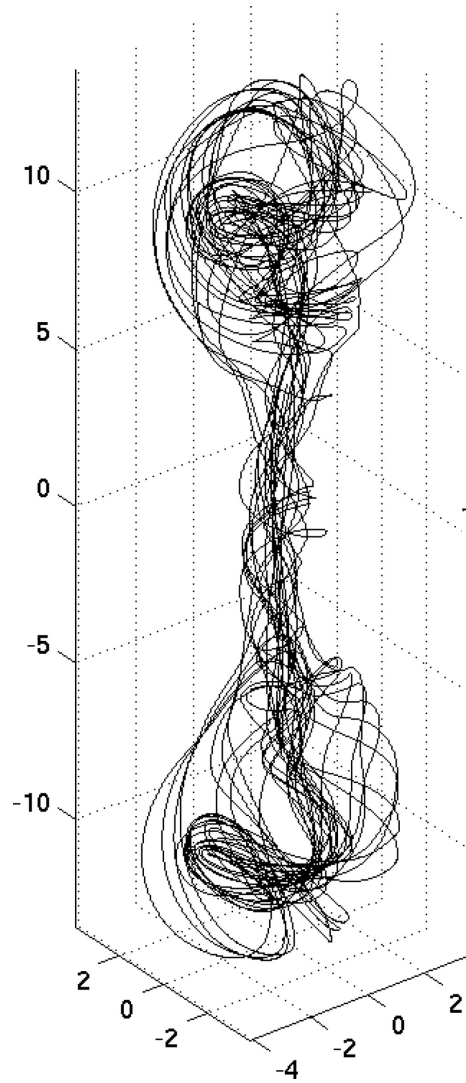
- Linear sizes
kpc - Mpc
- Ages
10 kyr - 100 Myr
- Total energies
 $10^{55} - 10^{62}$ erg
- Jet luminosities
 $10^{43} - 10^{47}$ erg/s
- Equipartition field
 $B_{eq} \sim 0.5 - 50 \mu\text{G}$

Predominantly Toroidal

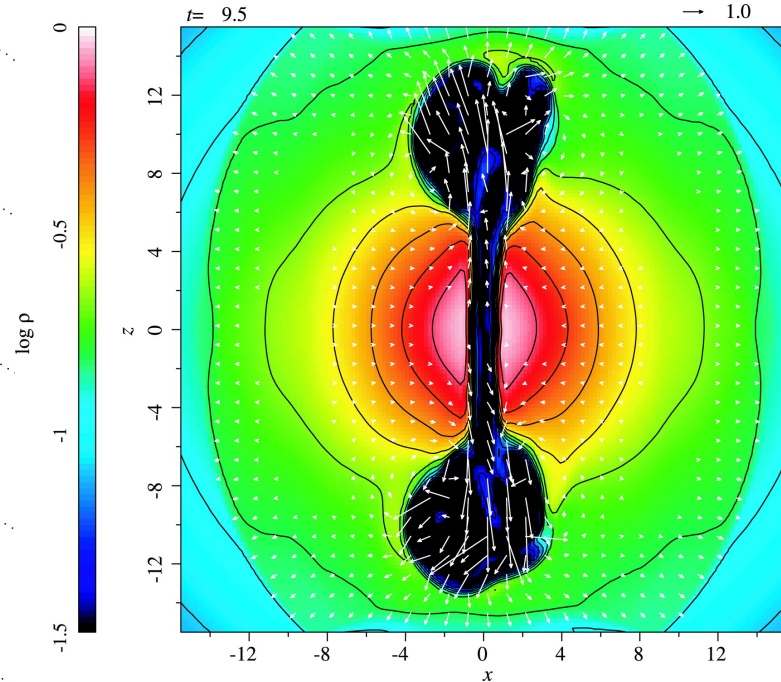


2D axisymmetric ideal MHD simulations of strongly magnetized jets with no substantial poloidal magnetic field: thin (“no-backflow”) cocoons and “nose-cone” morphology of jet termination regions (Lind et al. 1989)

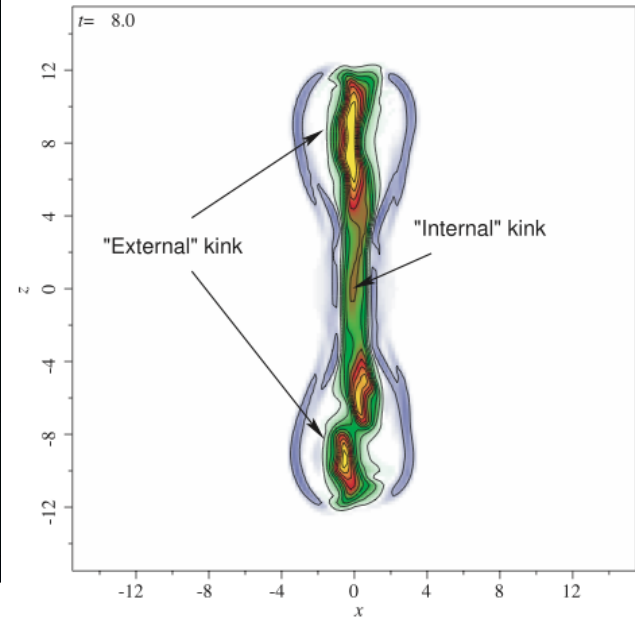
Large-Scale Helix?



Magnetic field lines



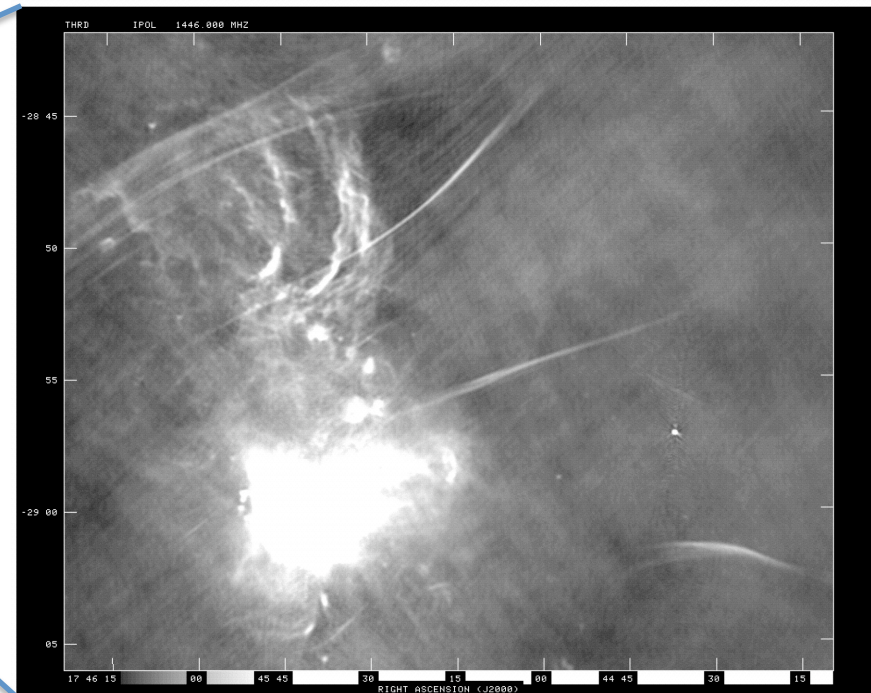
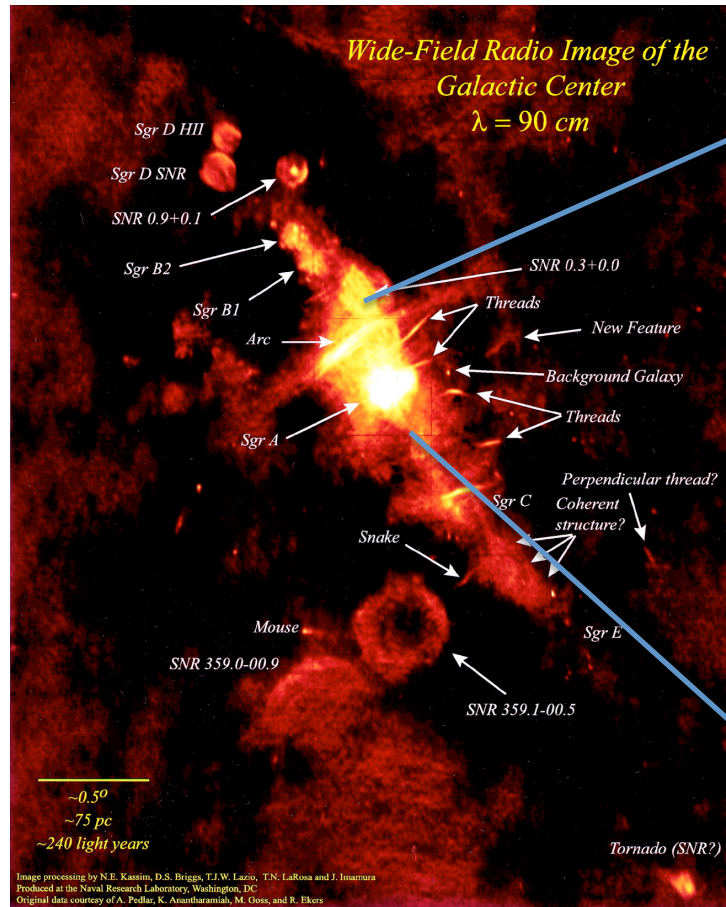
Density and poloidal velocity field



Current distribution

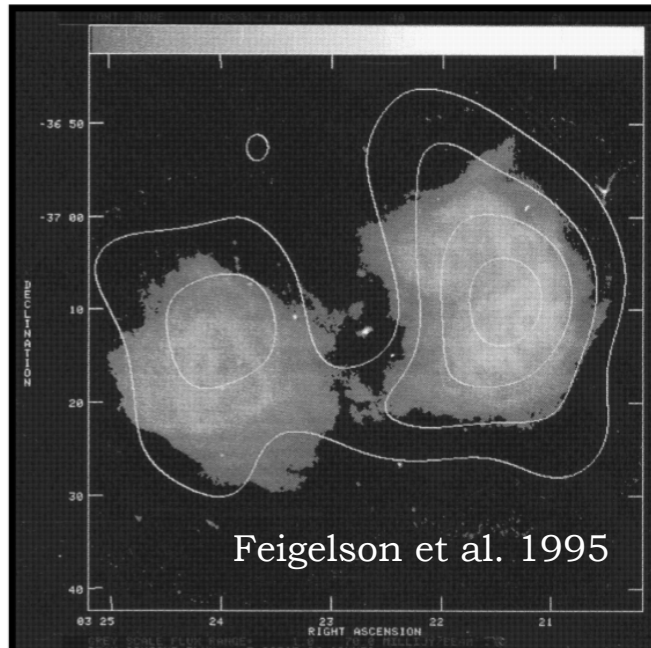
“Magnetic tower” jets have to be launched from the outer parts of the accretion disk in order to support strong poloidal magnetic field assumed (Li et al. 2006, Nakamura et al. 2006/08)

Radio Filaments Within CMZ



LaRosa et al. 2000: Galactic Center at 90 cm (4deg \times 2.5deg image with a resolution of 43" \times 24").
 “Radio Arc” (originally discovered by Yusef-Zadeh et al. 1984) and other linear strongly polarized filaments emitting flat-spectrum synchrotron emission (also Lang et al. 1999, LaRosa et al. 2001-04). The fundamental question is if the non-thermal filaments are tracers of a global large-scale magnetic field in the Galactic Center region. If so, and if this field is pervasive, the total energy in the poloidal component within the Central Molecular Zone would be as high as $E_B \geq 10^{55} \text{ erg}$

Lobes in X-rays

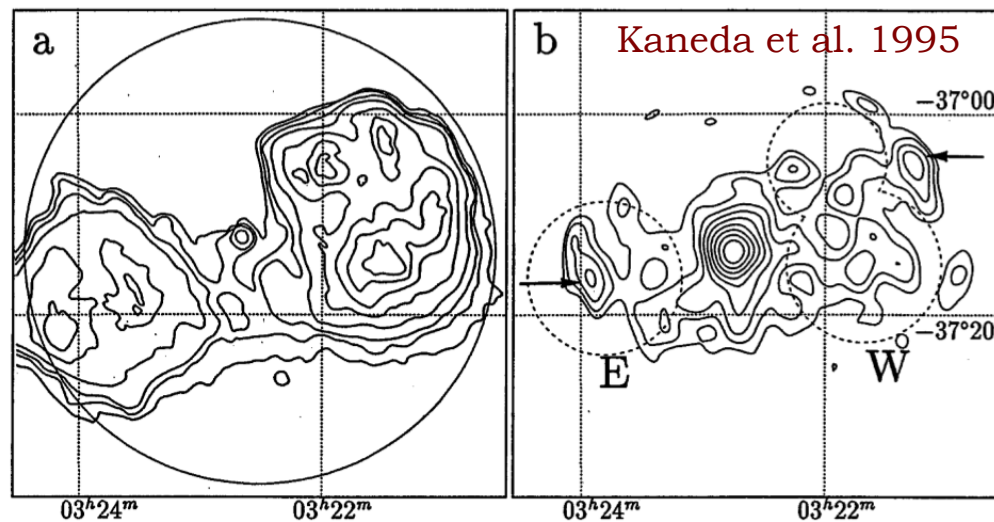


$$B_{\text{eq}}: U_B \approx U_e$$

Harris & Grindlay 1979:
the expected X-ray Inverse-Compton (IC/CMB) emission due to the radio-emitting GeV-energy electrons within the extended lobes

$$L_{\text{syn}} \sim U_B \times U_e \times V$$

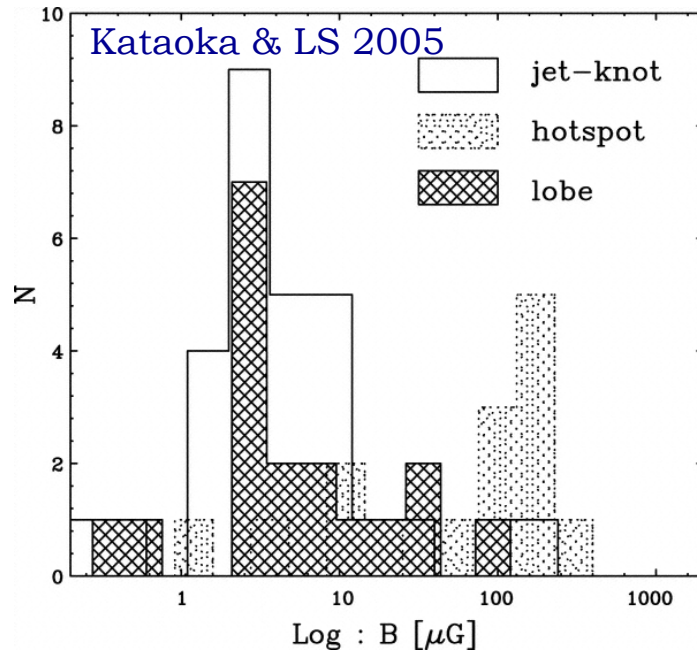
$$L_{\text{IC}} \sim U_{\text{cmb}} \times U_e \times V$$



First detection:
Fornax A with ROSAT and ASCA
(Feigelson et al. 1995, Kaneda et al. 1995)

$$U_e/U_B \approx 1$$

Chandra, XMM, Suzaku

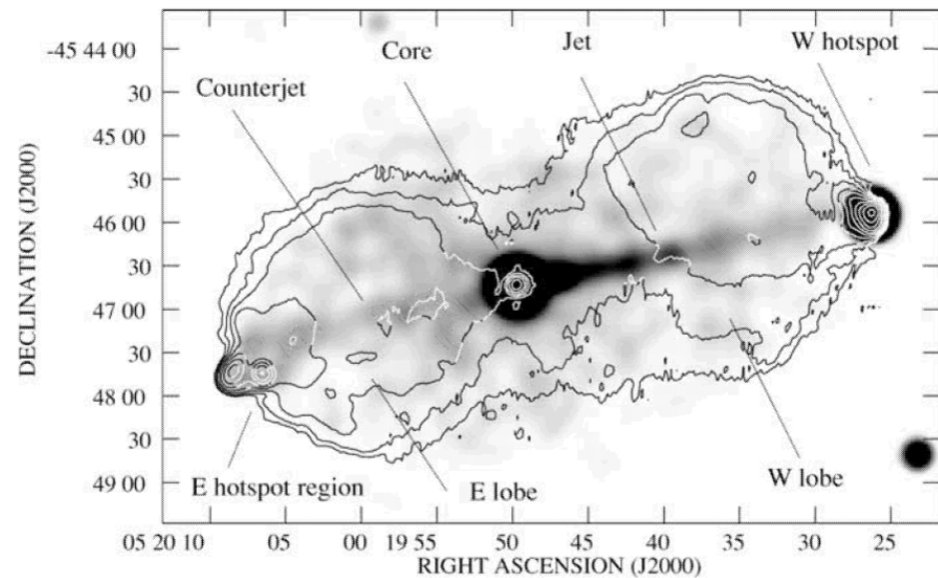
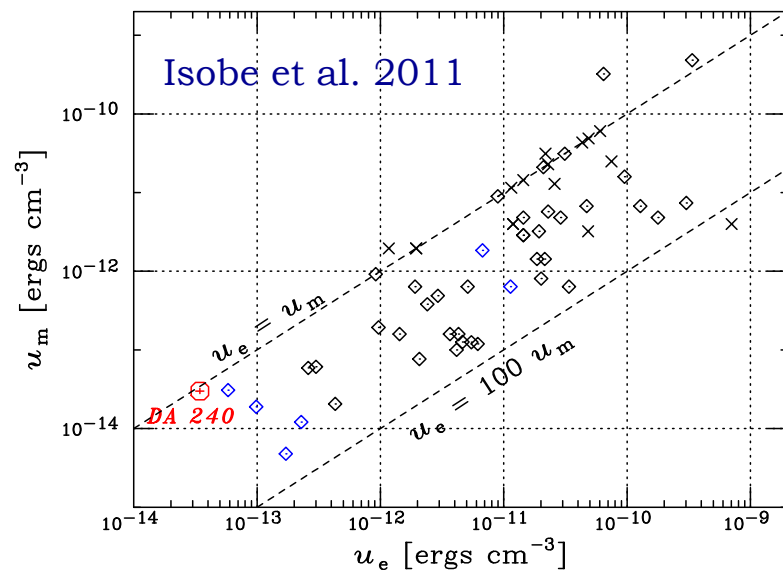


Systematic studies with modern high-resolution X-ray telescopes imply

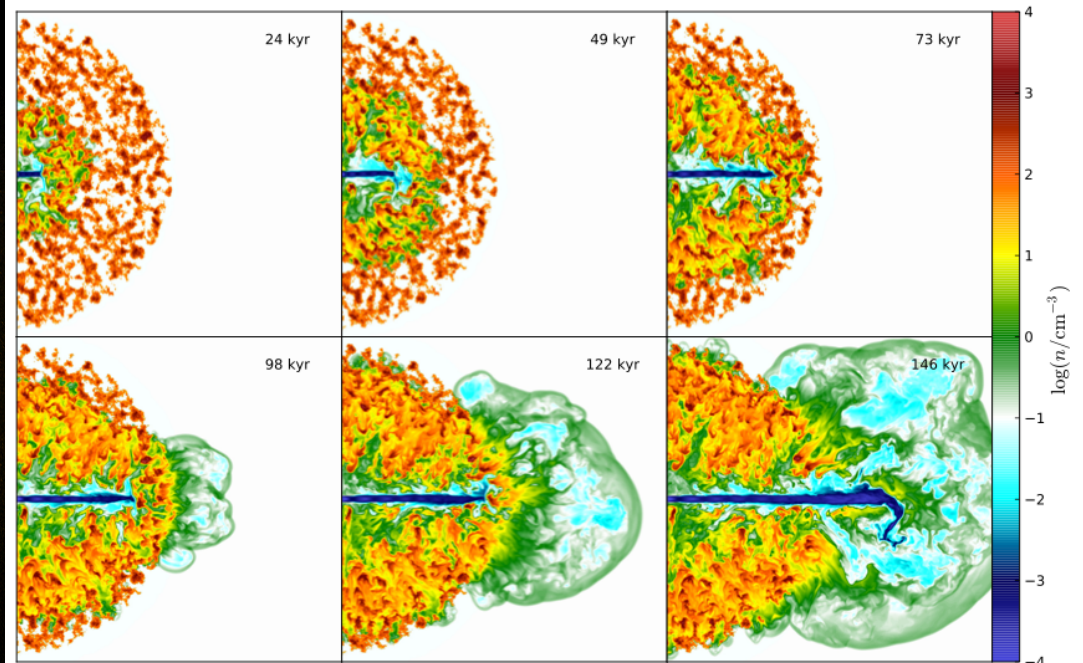
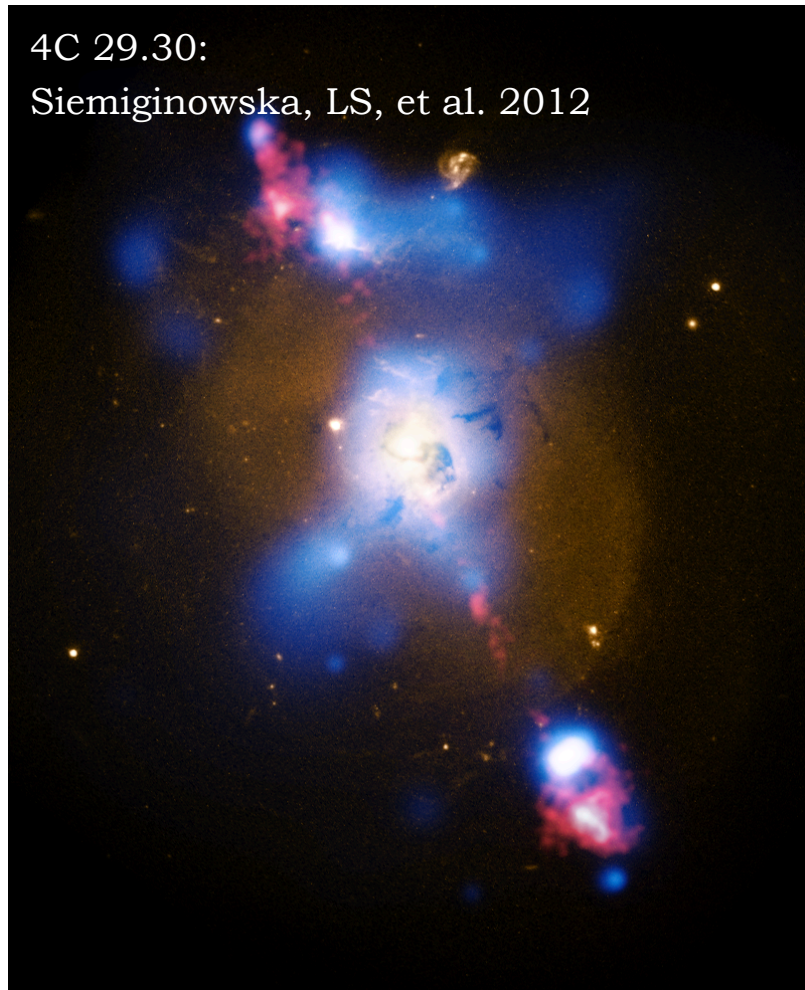
$$U_e/U_B \approx 1 - 100$$

assuming that all the detected X-ray photons are due to the IC/CMB emission (Kataoka & LS 2005, Croston et al. 2005, Isobe et al. 2011).

Only in a few cases photon statistics allows for a precise determination of the X-ray spectra (e.g., Pictor A: Hardcastle & Croston 2005).



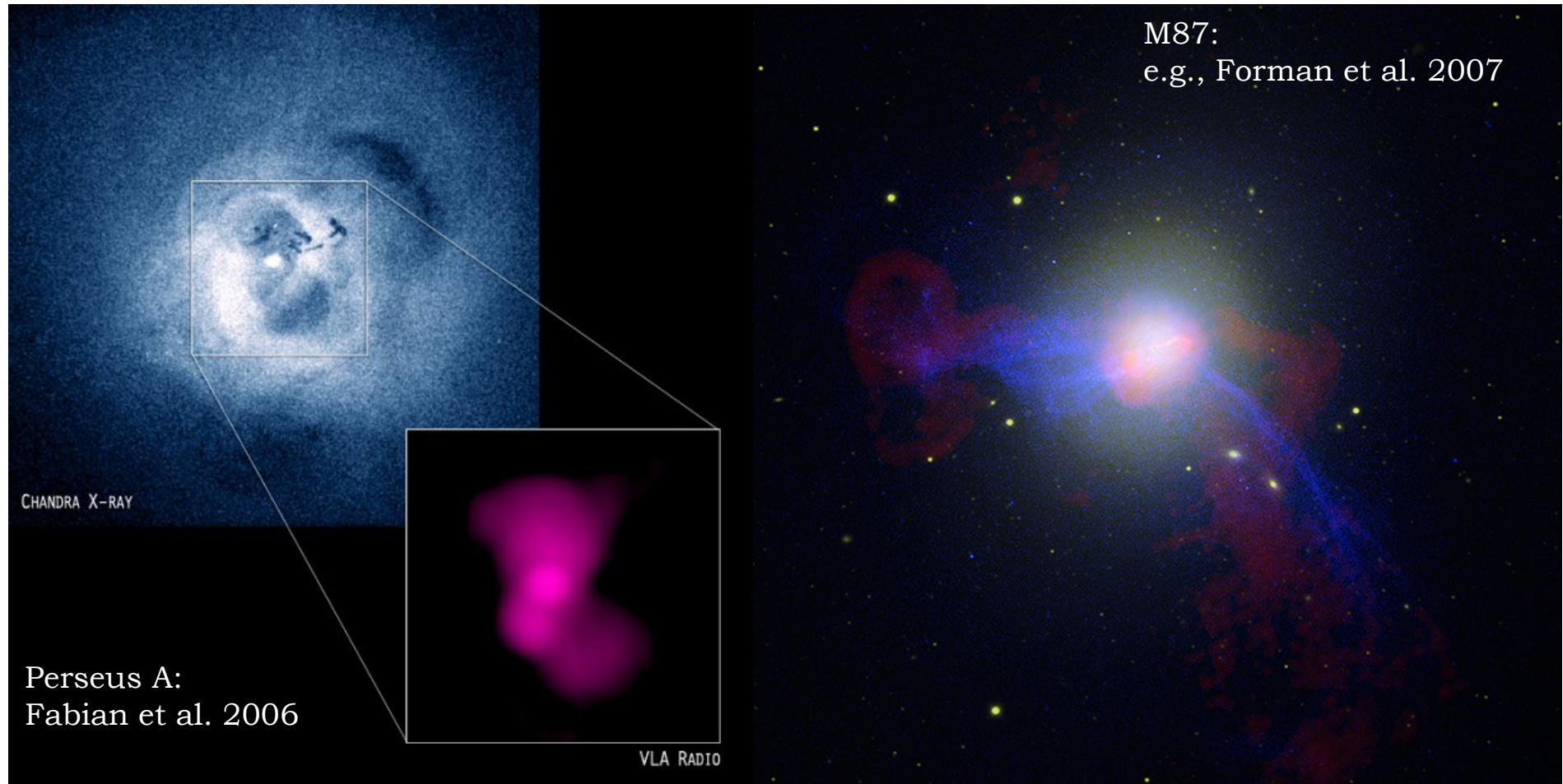
Jet-ISM Interactions



Wagner & Bicknell 2011:
interaction of a low-power jet with inhomogeneous,
clumpy ISM

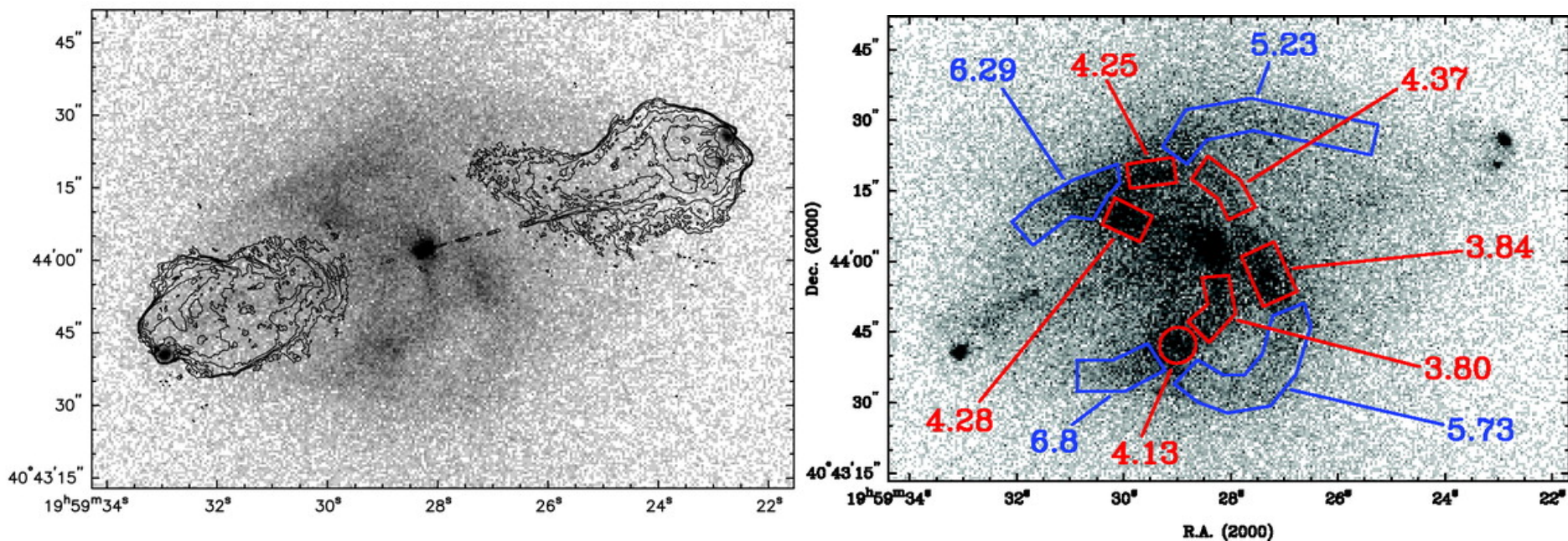
Complex MWL morphologies. X-ray observations suggest gaseous outflows driven by relativistic jets, as well as gas heating by weak shocks driven by the expanding lobes (-> feedback processes).

Jet-ICM Interactions



Similarly complex MWL morphologies. X-ray observations reveals gas mixing and heating due to the jet activity in radio galaxies located in the central parts of clusters (-> **feedback processes**).

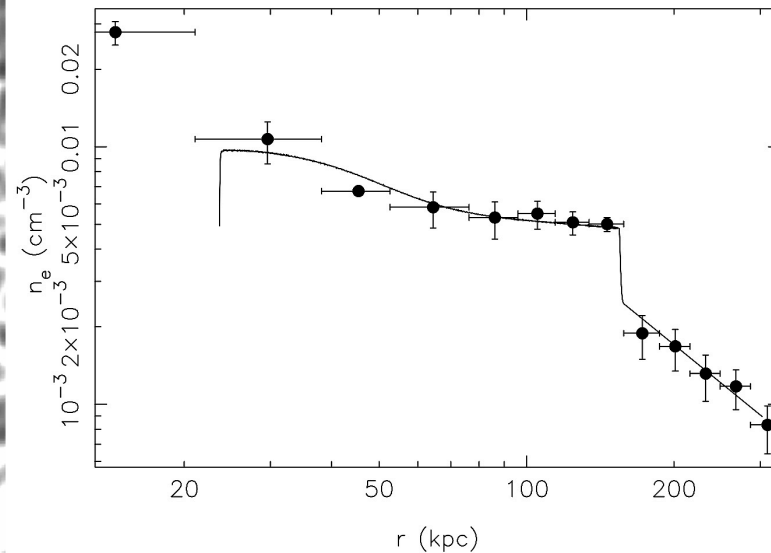
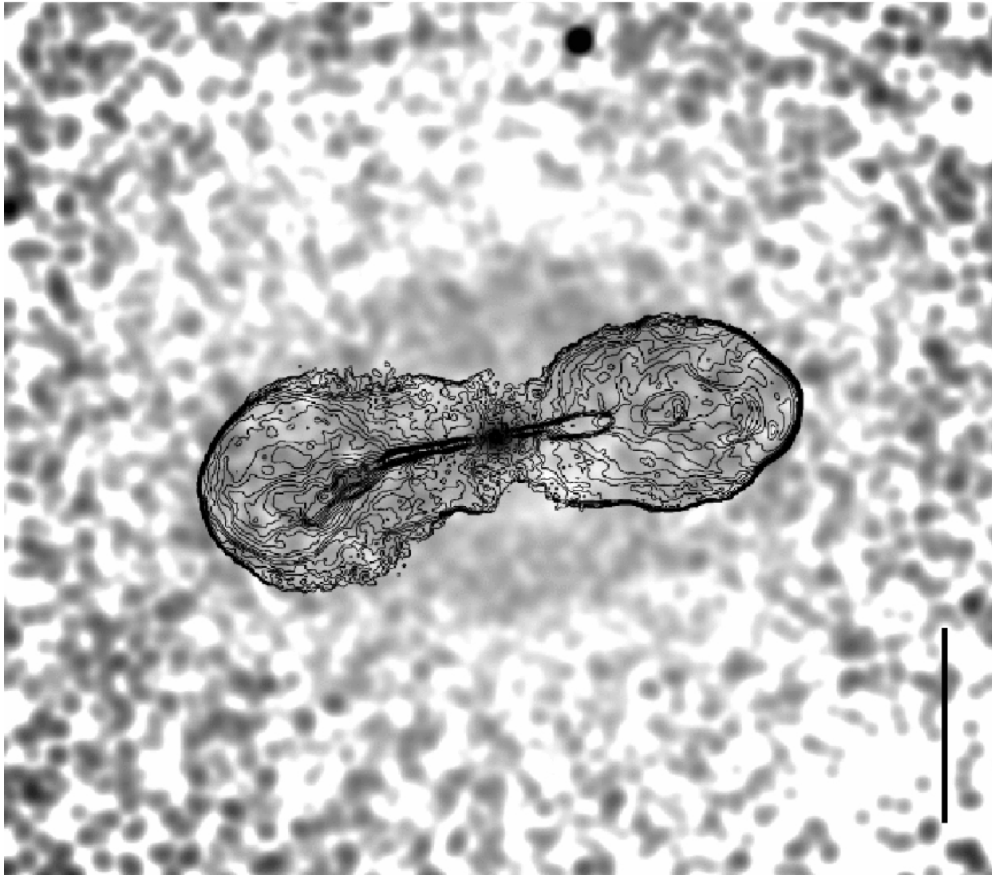
Jet-ICM Interactions



Wilson et al. 2006: limb-brightened cavity of the radio galaxy Cygnus A revealed by Chandra. The gas along the edges of the cavity is hotter than the adjacent ICM. This suggests a presence of weak shocks driven by the expanding lobes ($M \sim 1.3$).

Most of the power of the jets in Cygnus A is currently going into heating the ICM.

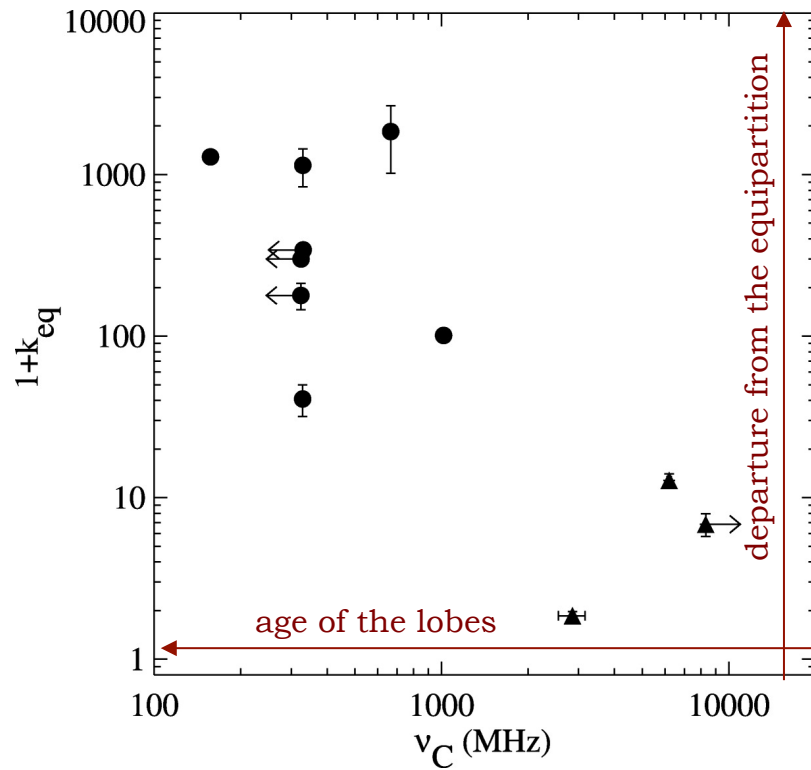
Jet-ICM Interactions



Nulsen et al. 2005 : Shock front around the lobes of the Hercules A radio galaxy residing in the center of a cooling flow cluster.

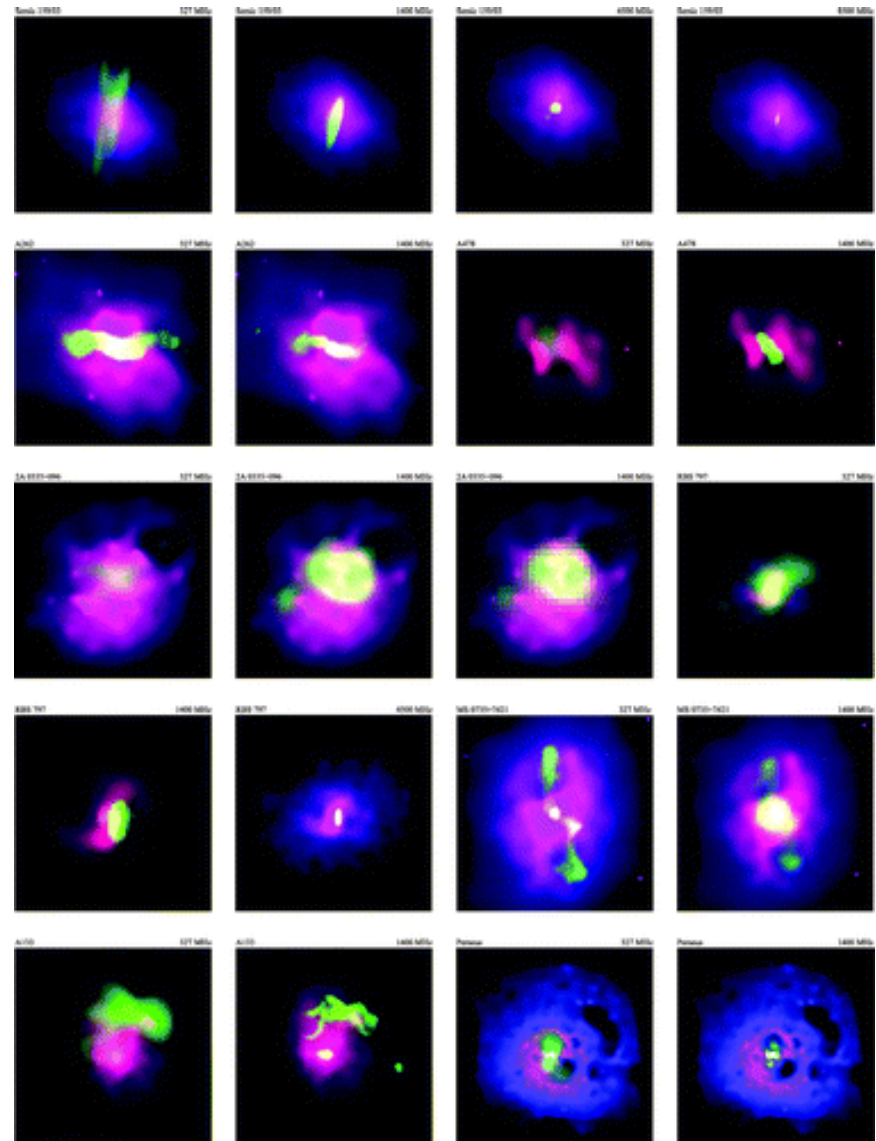
The shock has a Mach number of 1.65, making it the strongest of the cluster-scale shocks driven by an AGN outburst found so far. The age of the outburst is ~ 60 Myr, its energy $\sim 3 \times 10^{61}$ ergs, and its mean power $\sim 2 \times 10^{46}$ erg/s.

Protons?

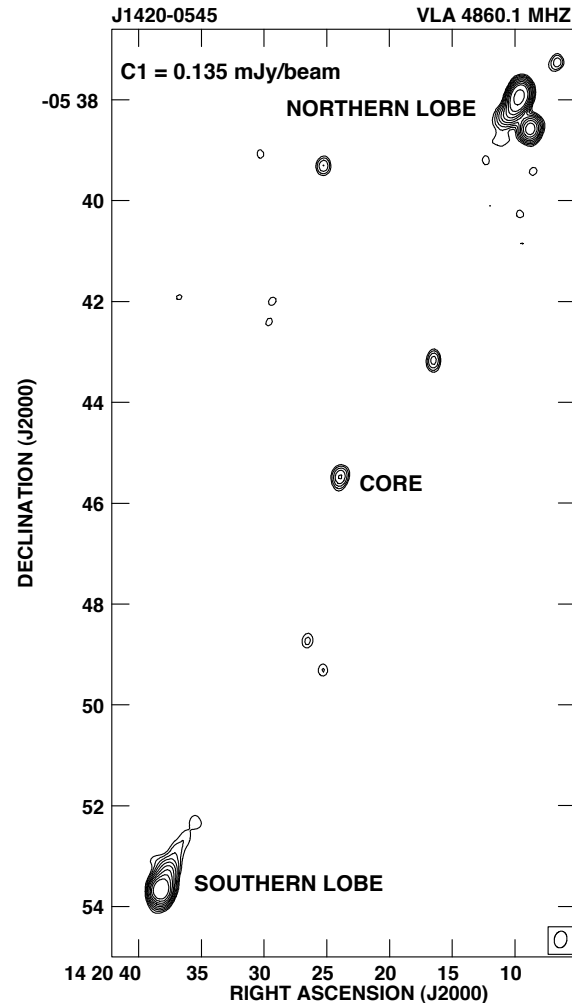


Birzan et al. 2008: kpc-scale lobes of low-power radio galaxies located at the centers of rich clusters cannot be supported solely by the pressure of the magnetic field and ultrarelativistic electrons.

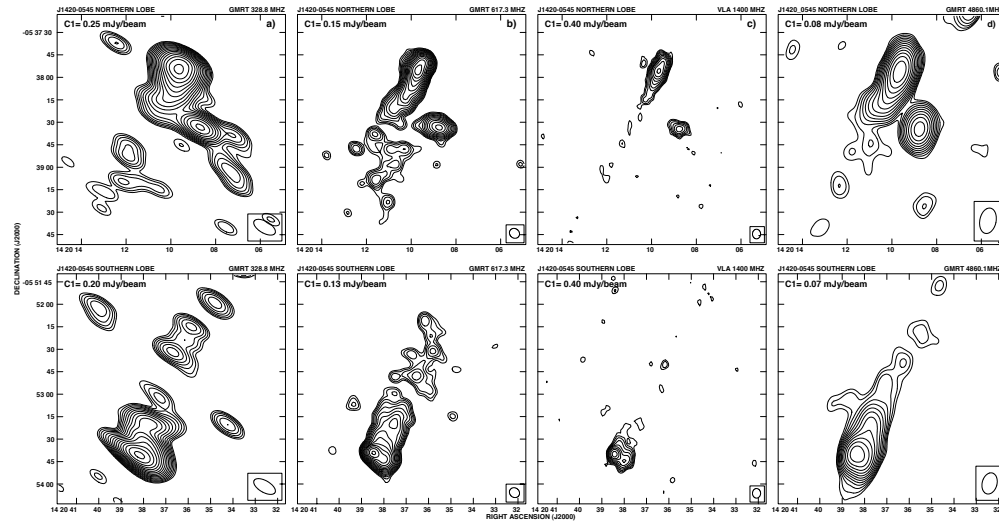
Entrained thermal gas, or relativistic protons?



Jet-IFM Interactions



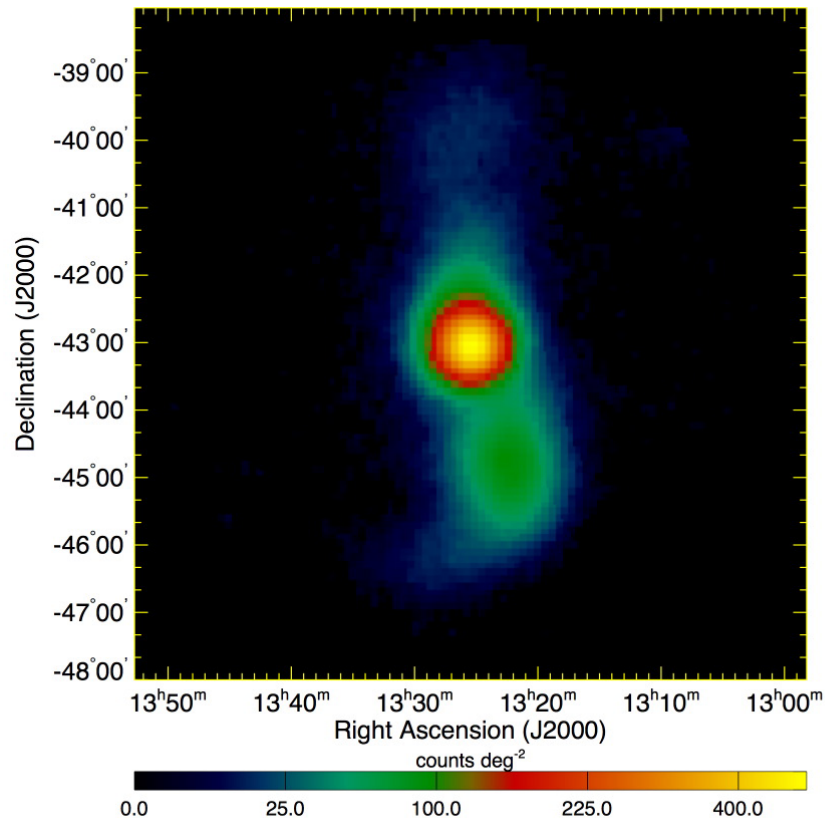
Machalski, Jamrozny, LS & Koziel, 2011



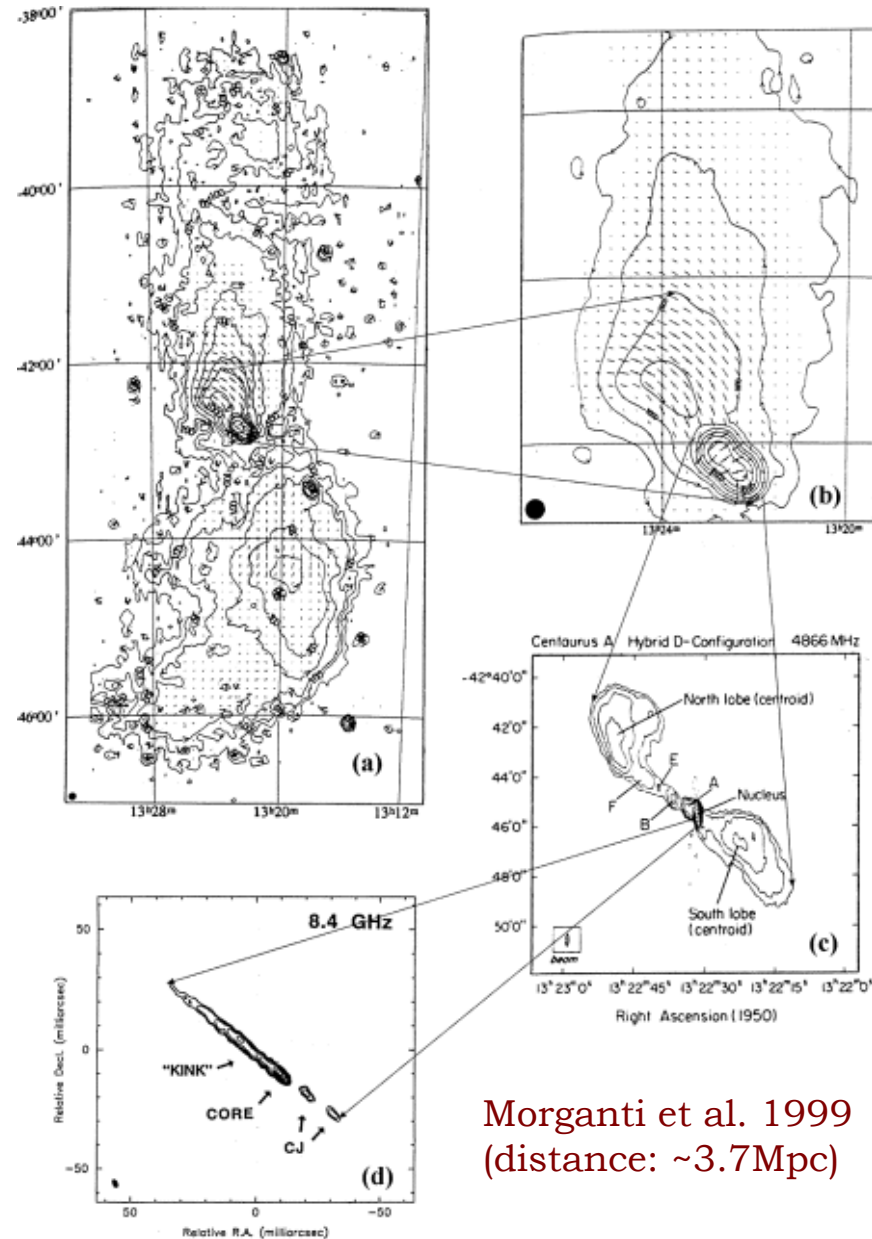
The largest radio galaxy known up to date
J1420-0545 with the total projected linear size of
4.69 Mpc (discovered by Machalski et al. 2008).

The extremely low density of the gas surrounding the lobes is consistent with the mean density of the baryonic matter in the Universe. This suggests that the source is located in a real void of the galaxy and matter distribution, and as such it modifies substantially the surrounding matter by driving strong shocks and heating the gas located at the outskirts of the filamentary galactic distribution.

Complex Structure of Cen A

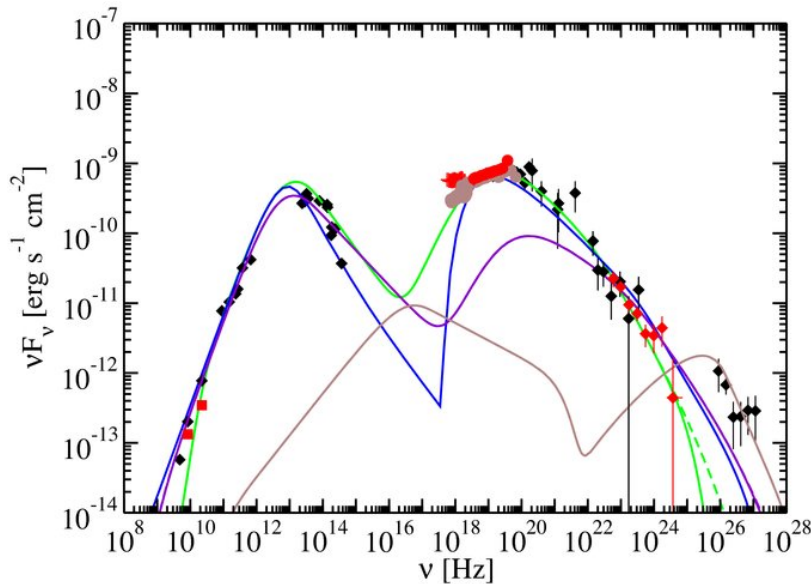
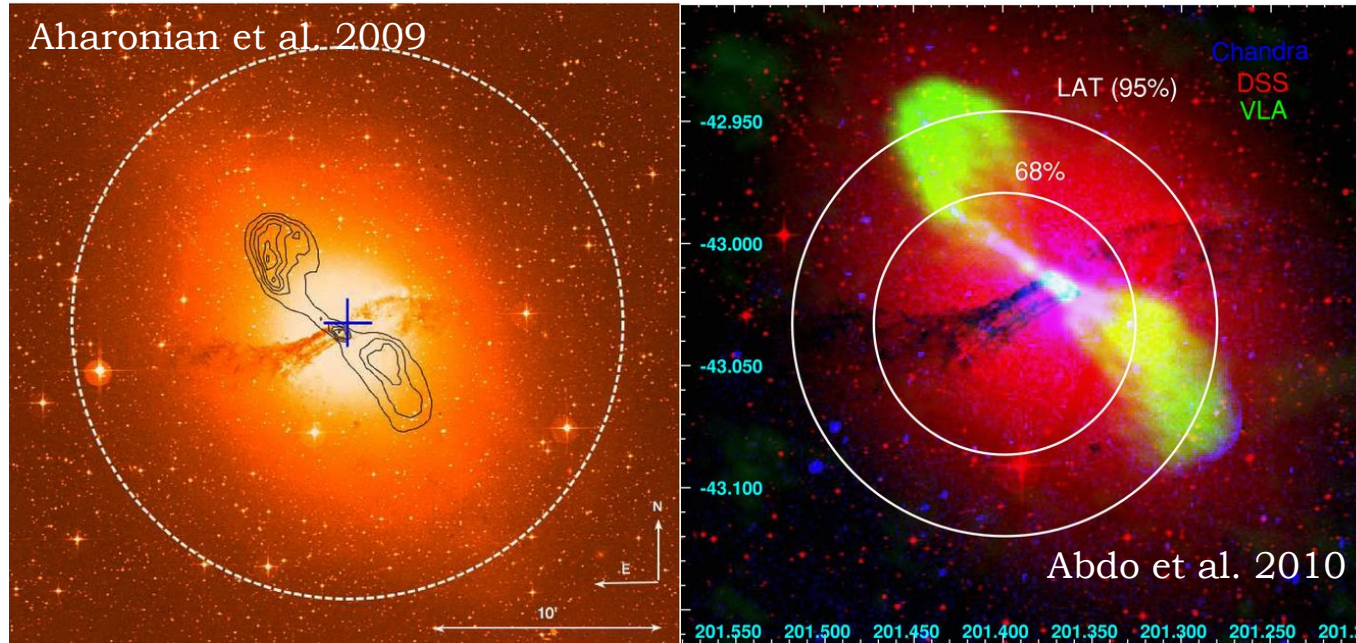


Giant lobes in Centaurus A resolved by WMAP (Hardcastle et al. 2009)
lifetime ~ 30 Myr, scale ~ 600 kpc



Morganti et al. 1999
(distance: ~ 3.7 Mpc)

Active Nucleus

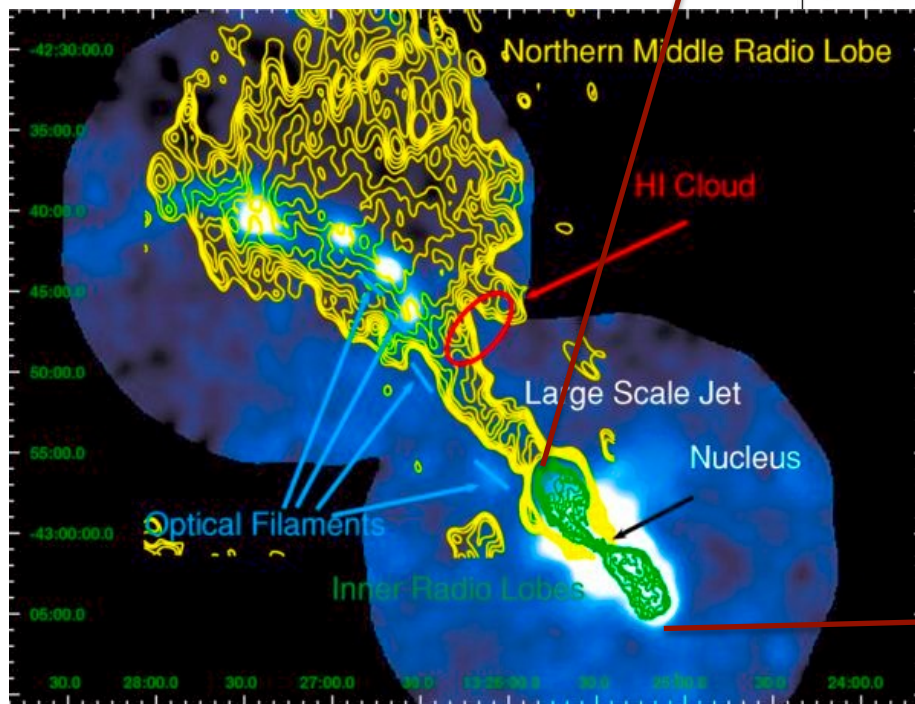


Central regions of Centaurus A have been detected in gamma-rays by all the instruments onboard CGRO, and more recently by H.E.S.S. and Fermi-LAT in the GeV-TeV ranges.

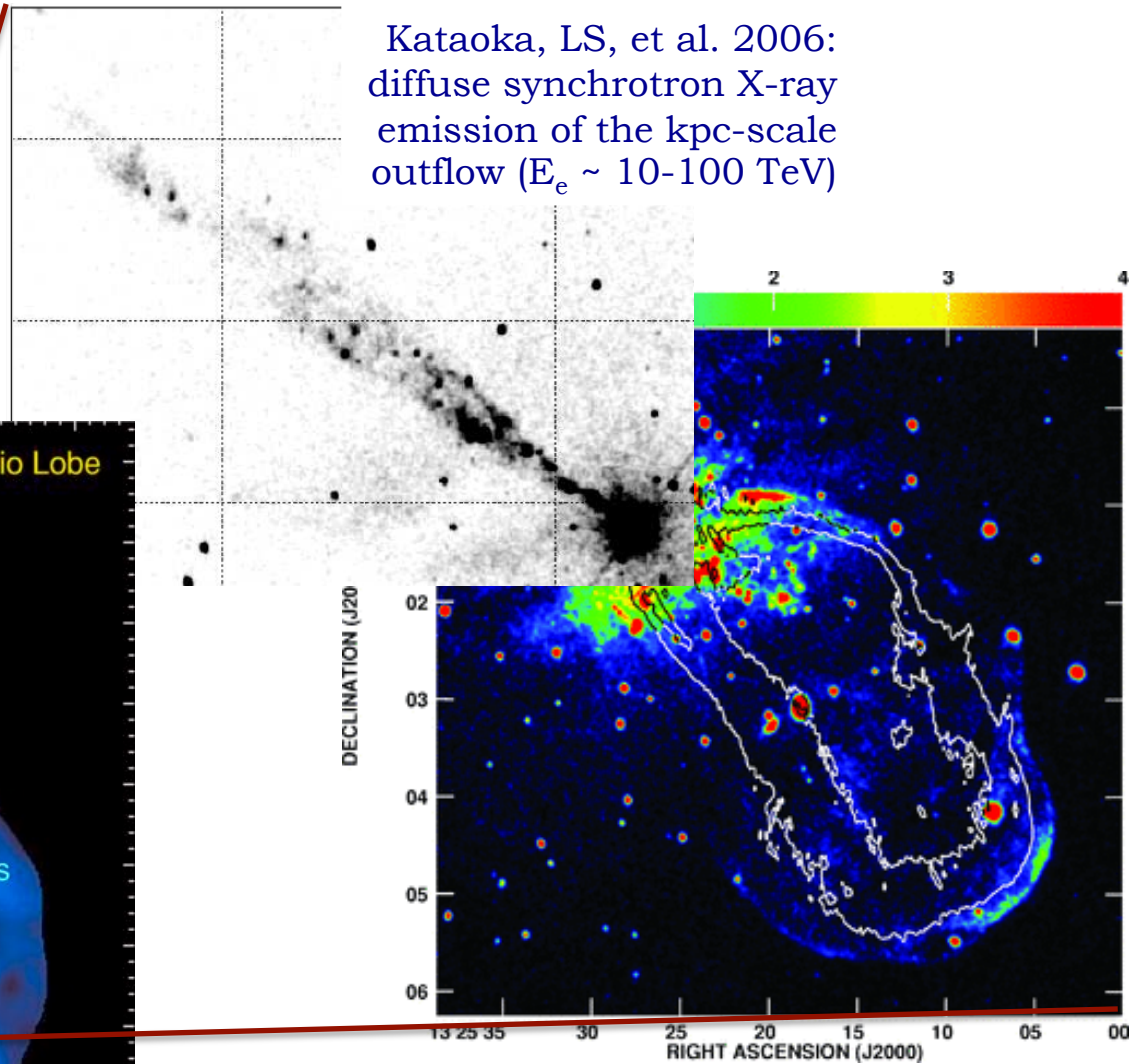
Modeling of the broad-band emission of the unresolved core in the framework of the “misaligned blazar” models (Abdo et al. 2010).

Large-Scale Structures

Kraft et al. 2009: clumps and filaments of the X-ray emitting thermal gas apparently heated by the expanding outflow.



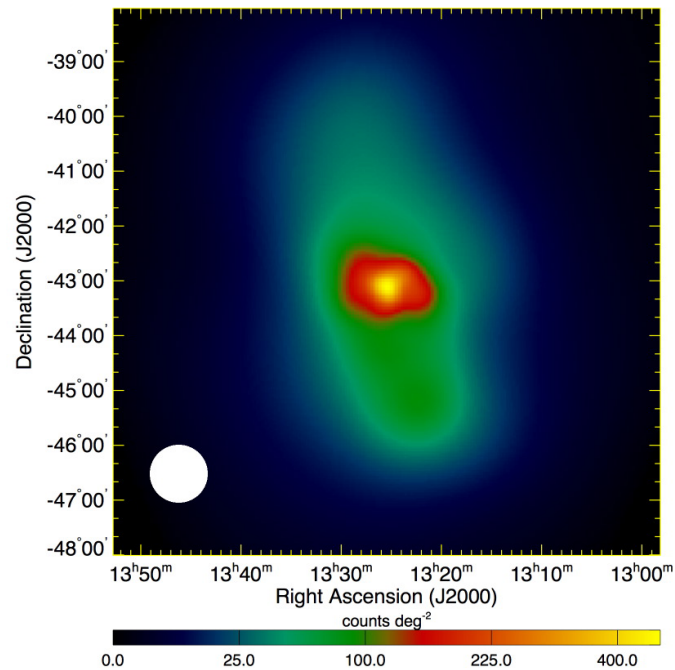
Kataoka, LS, et al. 2006: diffuse synchrotron X-ray emission of the kpc-scale outflow ($E_e \sim 10\text{-}100$ TeV)



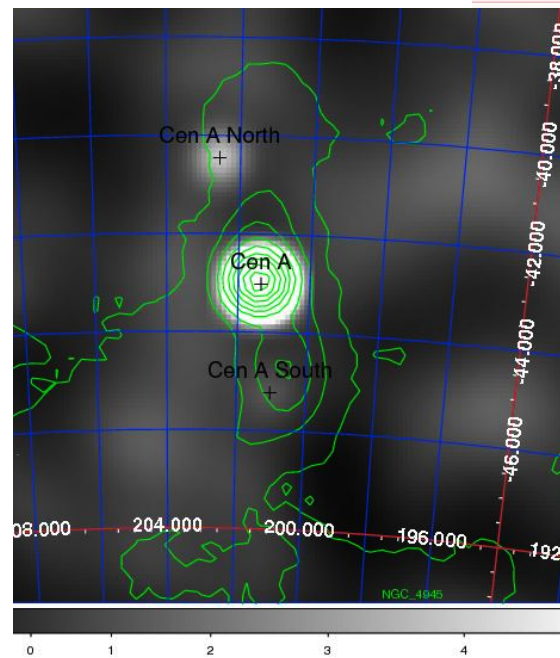
Croston et al. 2009: strong shock driven by the expanding inner kpc-scale southern lobe ($M_{sh} \sim 8$).

Giant Structure

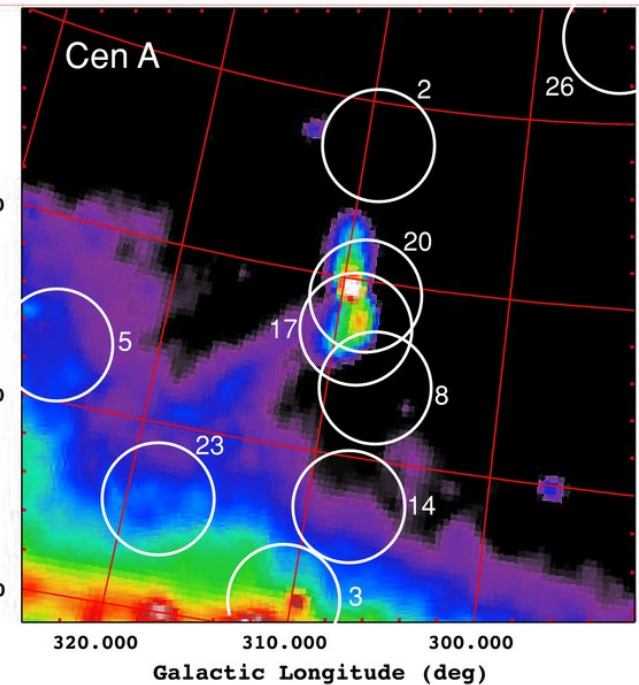
Abdo et al. 2010



Beckmann et al. 2011

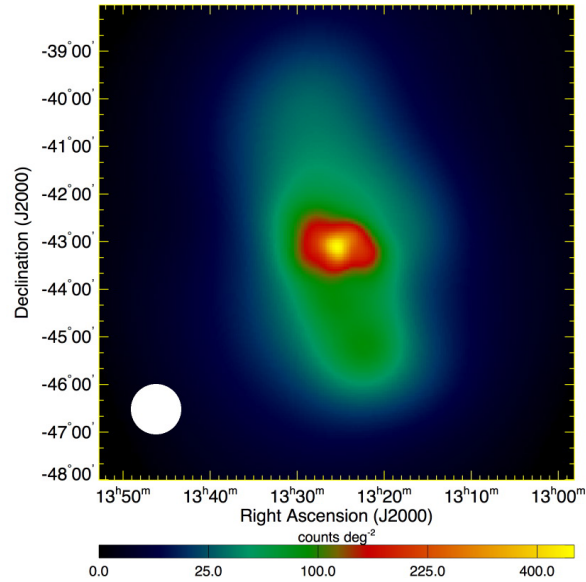


Moskalenko, LS, et al. 2009



- Fermi-LAT:** giant halo provides $\frac{1}{2}$ of the 0.1-100GeV luminosity of the entire system, $L_{\gamma} \sim 10^{41}$ erg/s
- INTEGRAL/SPI:** upper limits for the 0.04-1 MeV emission of the giant halo
- PAO:** association of the detected UHECRs with giant halo implies $L_{\text{UHE}} \sim 10^{39}$ erg/s

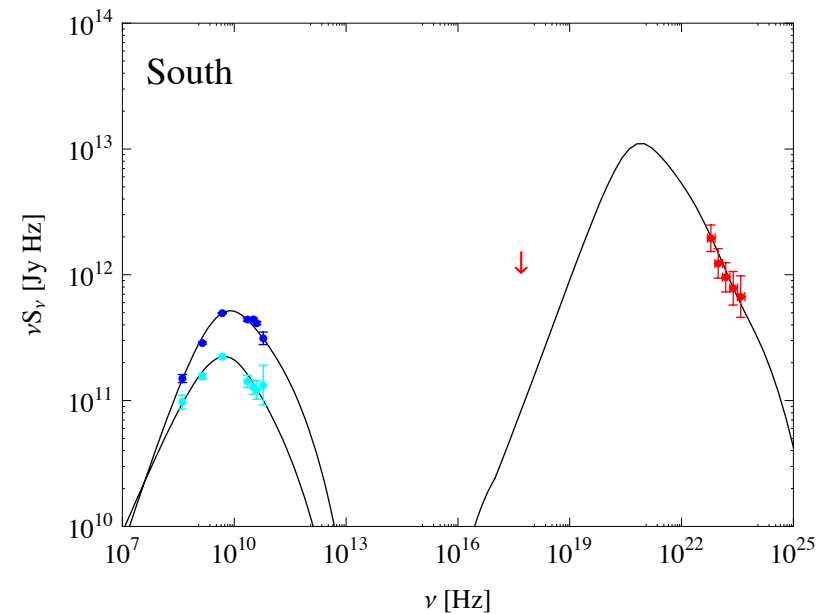
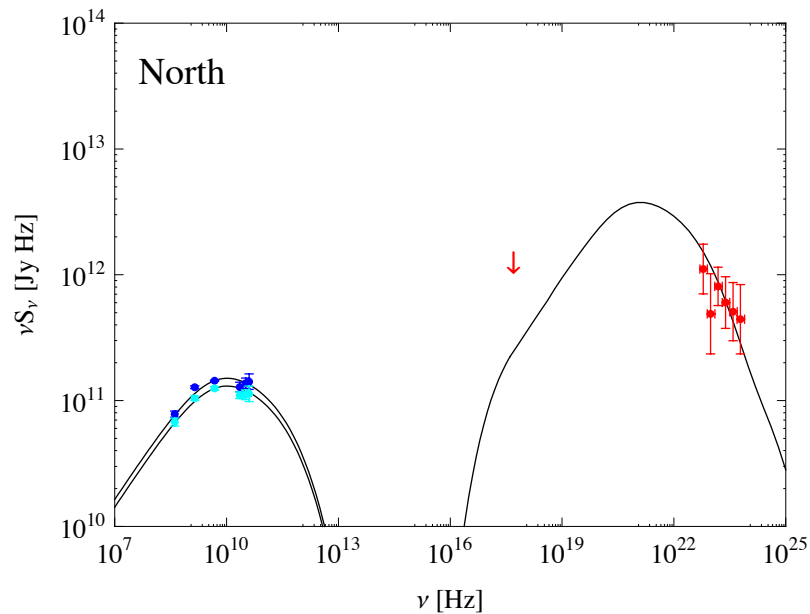
Fermi-LAT Imaging



IC/(CMB+EBL) fits the Fermi/LAT spectra:

$$\begin{aligned} B &\sim 1 \mu\text{G} \\ U_e/U_B &\sim 3 \\ E_{\text{tot}} &= 10^{58} \text{ erg} \\ L_j &\sim 10^{43} \text{ erg/s} (\sim 10^{-3} L_{\text{edd}}) \end{aligned}$$

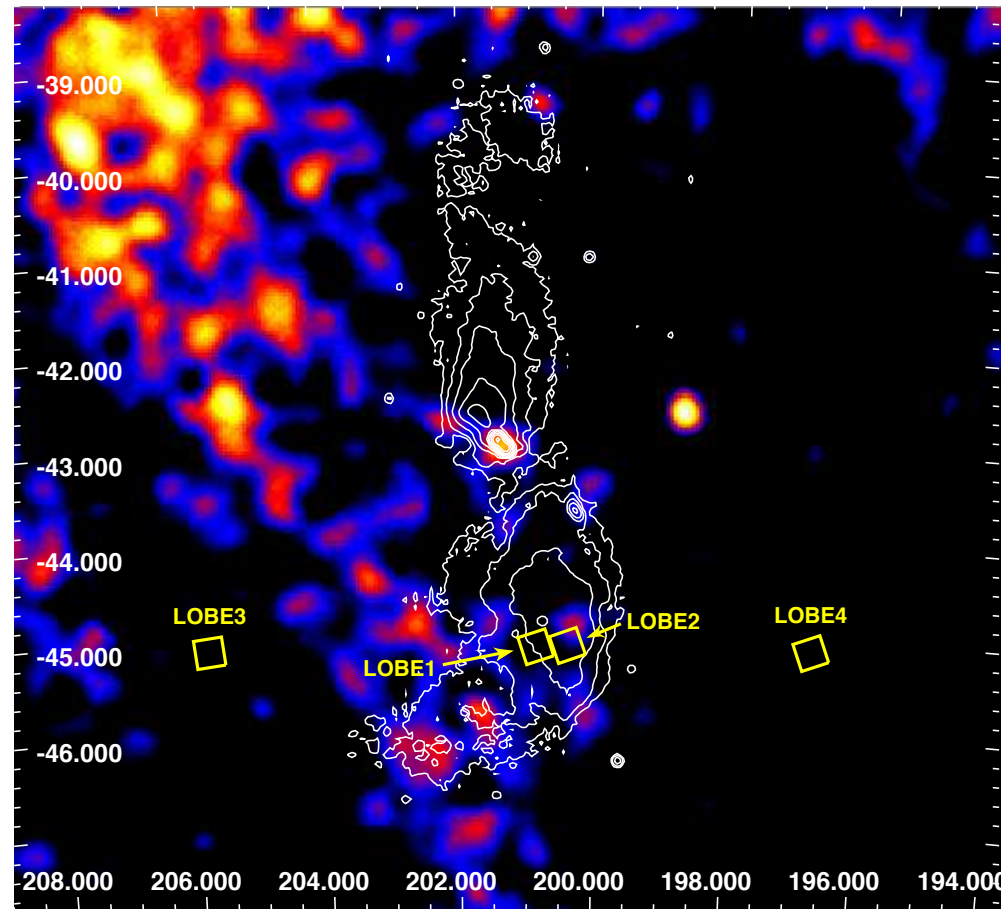
Abdo et al. 2010, Science
(CAs: Cheung, LS, Fukazawa & Knodlseder)



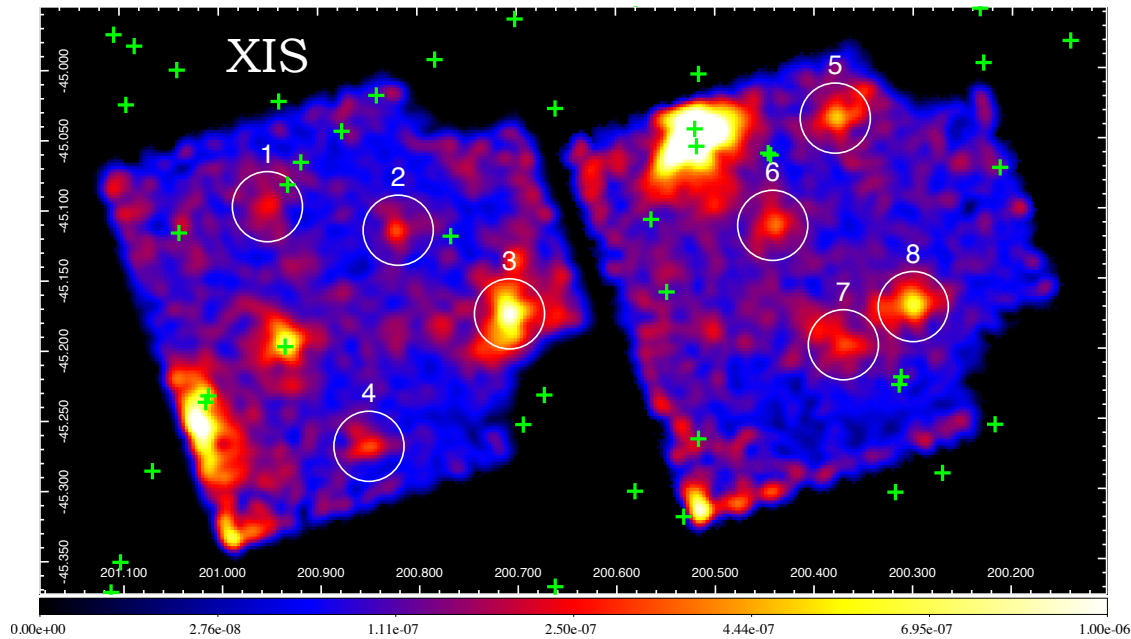
New Suzaku Observations

LS et al. 2012

Very first Suzaku observations of the southern giant lobe of Cen A. The low and relatively constant instrumental background of Suzaku/XIS is ideally suited for observations of low-surface brightness diffuse sources such as Cen A giant lobes. In addition, the spatial resolution of the Suzaku's XIS ($2'$) is well matched to the recently obtained high-resolution ($50''$) radio maps of the giant lobes, while the FOV of the instrument ($1/3 \text{ deg} \times 1/3 \text{ deg}$) is large enough to encapsulate within a single Suzaku pointing the large-scale structures (shells/filaments) revealed by the radio polarization maps



Point-Like Features



Unrelated foreground (stars) and background (AGN) sources.

“Possibly related” X-ray features: those with no obvious counterparts at other wavelengths (optical, infrared).

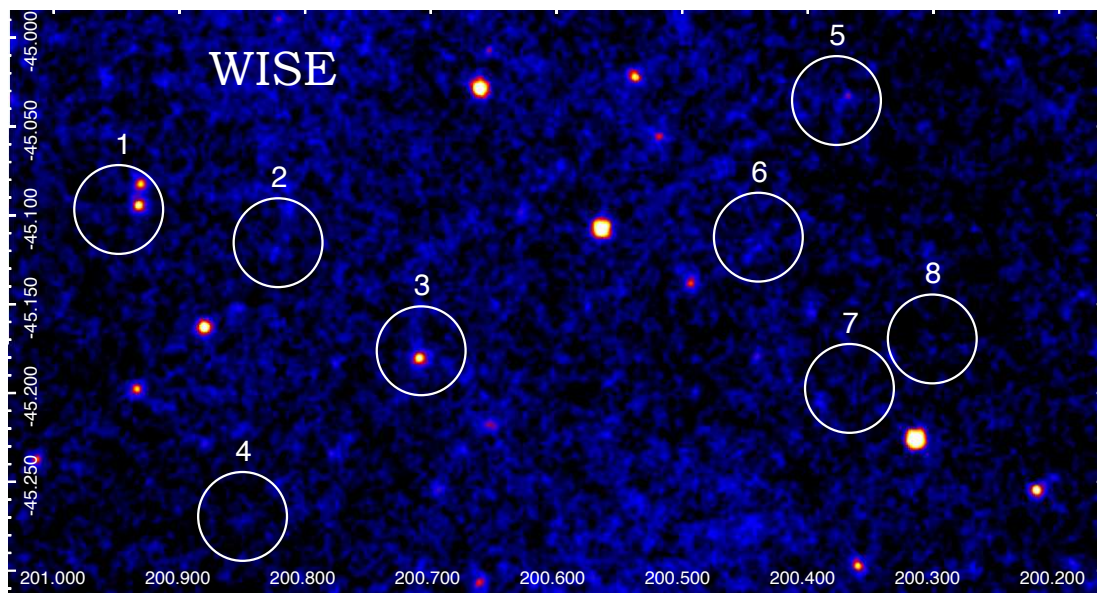
Total X-ray fluxes/luminosities of the “possibly related” features are not negligible:

$$F_x \sim 10^{-13} \text{ erg/cm}^2/\text{s}$$
$$L_x \sim 10^{38} \text{ erg/s}$$

per spot, on average

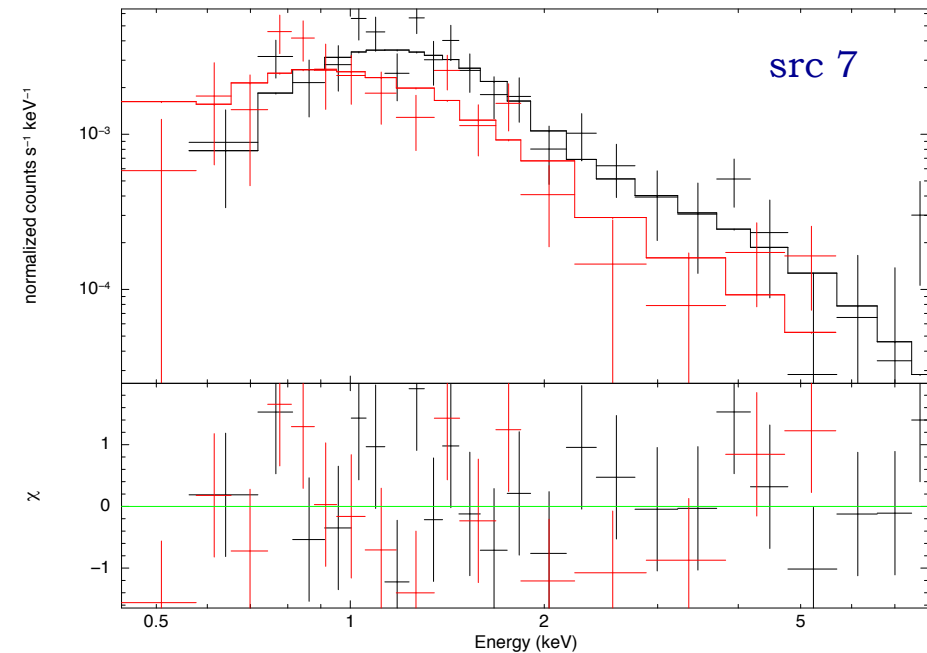
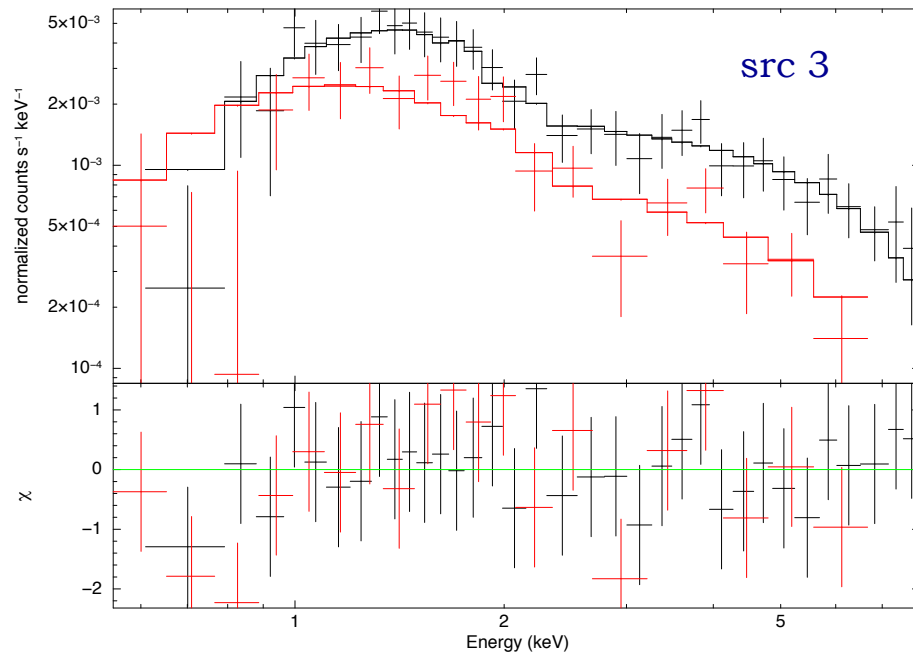
$$F_x \sim 3 \times 10^{-11} \text{ erg/cm}^2/\text{s}$$
$$L_x \sim 5 \times 10^{40} \text{ erg/s}$$

for the entire giant halo

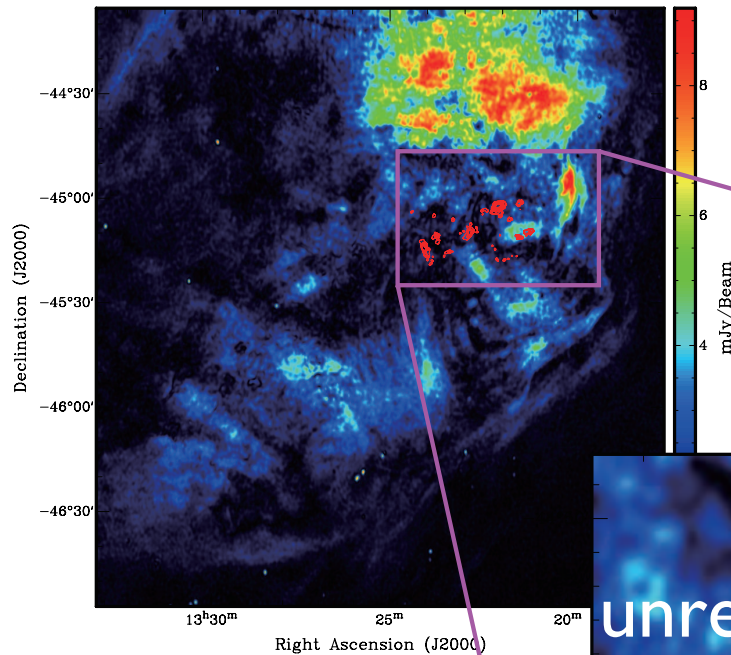


Spectral Analysis

source	red. χ^2 /dof	Γ	$F_{x, \text{abs}}$	F_x	red. χ^2 /dof	kT	$F_{x, \text{abs}}$	F_x	Z/Z_\odot	Norm	red. χ^2 /dof
(1)	(2)	(3)	(4)	(5)	(6)	(7)	(8)	(9)	(10)	(11)	(12)
src 3	1.340/8	$1.32^{+0.12}_{-0.12}$	29.2	30.4	0.671/51	32.8	28.3	29.5	0.3^f	$17.1^{+3.6}_{-2.2}$	0.639/52
src 5	0.211/8	$2.00^{+0.35}_{-0.32}$	6.6	7.3	1.192/30	$4.6^{+4.7}_{-1.6}$	6.3	6.8	0.3^f	$4.77^{+0.81}_{-0.82}$	1.249/31
src 6	0.395/8	$1.89^{+0.24}_{-0.21}$	7.5	8.3	0.804/36	$4.6^{+2.6}_{-1.3}$	6.9	7.4	0.3^f	$5.24^{+0.66}_{-0.67}$	0.788/37
src 7	0.693/8	$2.52^{+0.24}_{-0.23}$	7.1	8.3	1.020/38	$2.1^{+0.7}_{-0.3}$	5.8	6.5	0.3^f	$6.55^{+0.69}_{-0.69}$	1.373/39
src 8	0.598/8	$1.68^{+0.14}_{-0.14}$	15.8	16.8	0.685/47	$7.3^{+4.3}_{-2.1}$	14.9	15.8	0.3^f	$9.57^{+0.73}_{-0.71}$	0.770/48

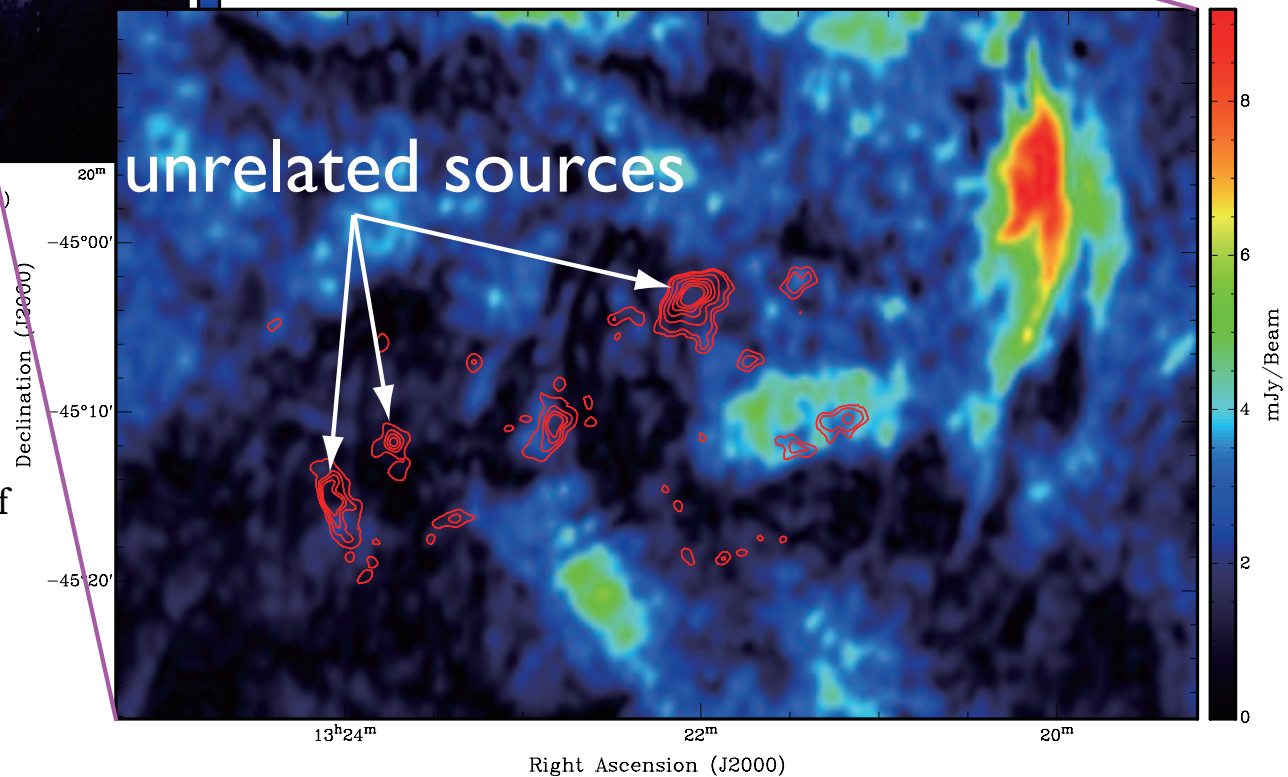


Related?

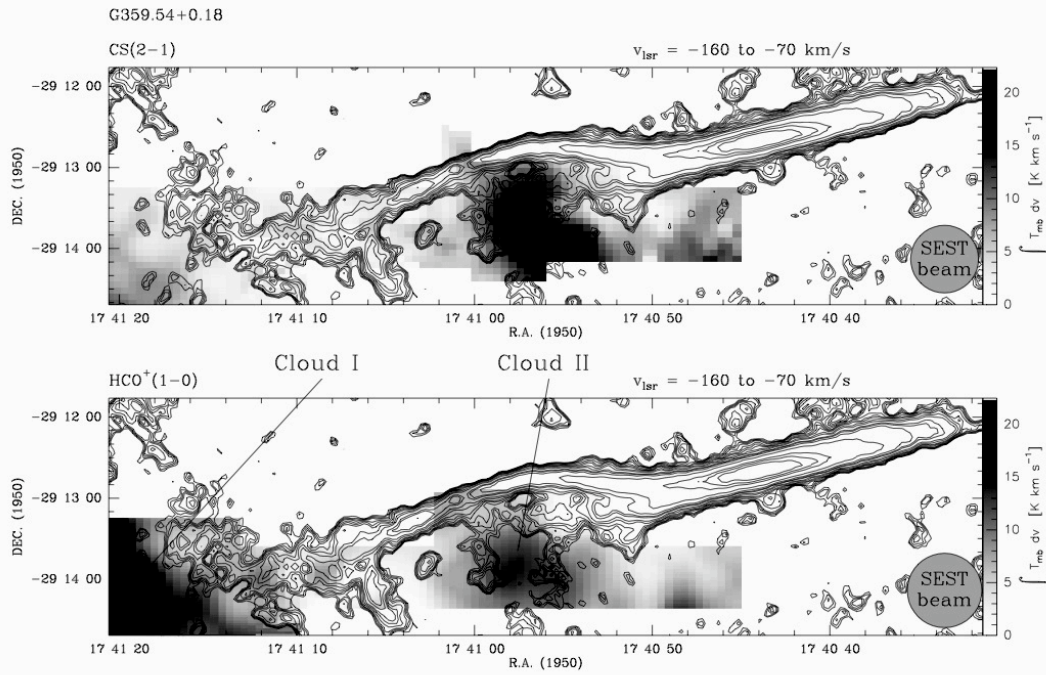


THERMAL: the energy of the reconnecting magnetic field, released primarily in the form of short-scale magnetic turbulence, is used to heat the plasma of the interacting gaseous condensation, and to form in this way the observed compact X-ray-emitting features.
BUT: thermal spots would have to be over-pressured by orders of magnitude!

NON-THERMAL: the magnetic energy released locally at the locations of reconnecting magnetic tubes/radio filaments is responsible for the confinement and acceleration of synchrotron X-ray emitting electrons within distinct emission sites up to 100 TeV energies.
BUT: very efficient acceleration process required



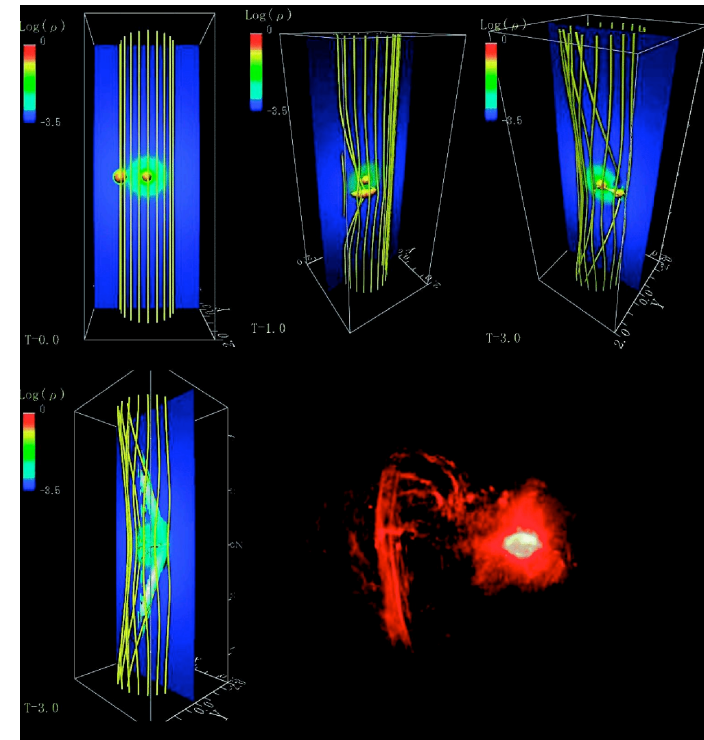
Galactic Filaments Again



Grey scale: Integrated molecular line intensity over the velocity range as specified above
 Contours: Continuum flux at 5GHz: Levels [mJy/beam]: .15, .2, .25, .3, .4, .5, .6, .8, 1.0, 1.2, 1.4, 1.6, 2.0, 3.0, 5.0, 6.0, 7.0

Staguhn et al. 1998:

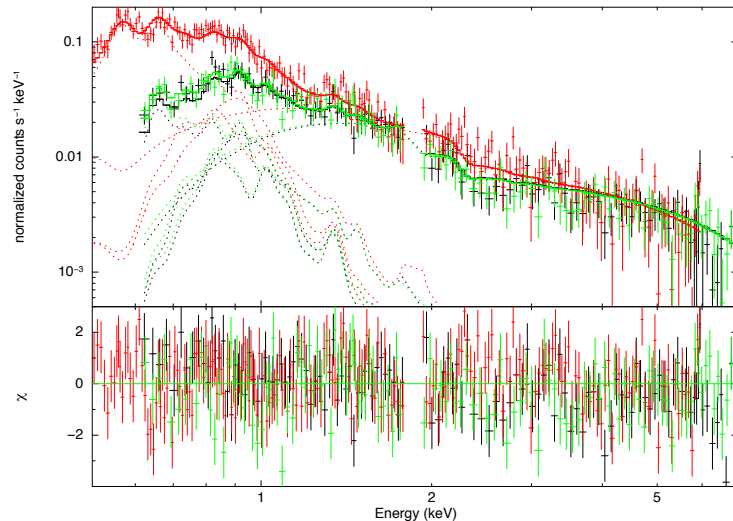
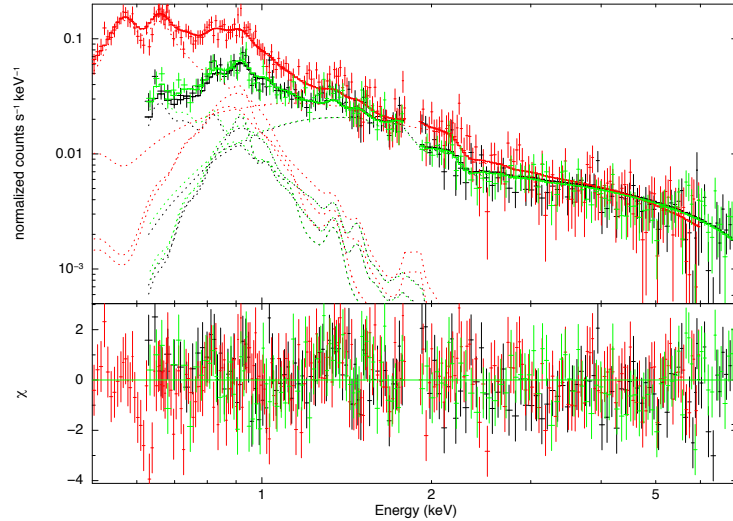
Endpoints of several filaments coincide with molecular clumps, suggesting that magnetic energy is liberated as the ambient field, tangled by the clumps' motions, reconnects in the advancing clumps' leading, externally ionized surface layer.



Sofue et al. 2005:

Three-dimensional, non-axisymmetric MHD simulation of the interaction of a gas cloud with a vertical magnetic field in the Galactic Center region. The field is embedded in a hydrostatic gaseous halo around a central mass. The moving cloud is disturbed by the gravitation, and locally twists the magnetic field.

Diffuse Excess

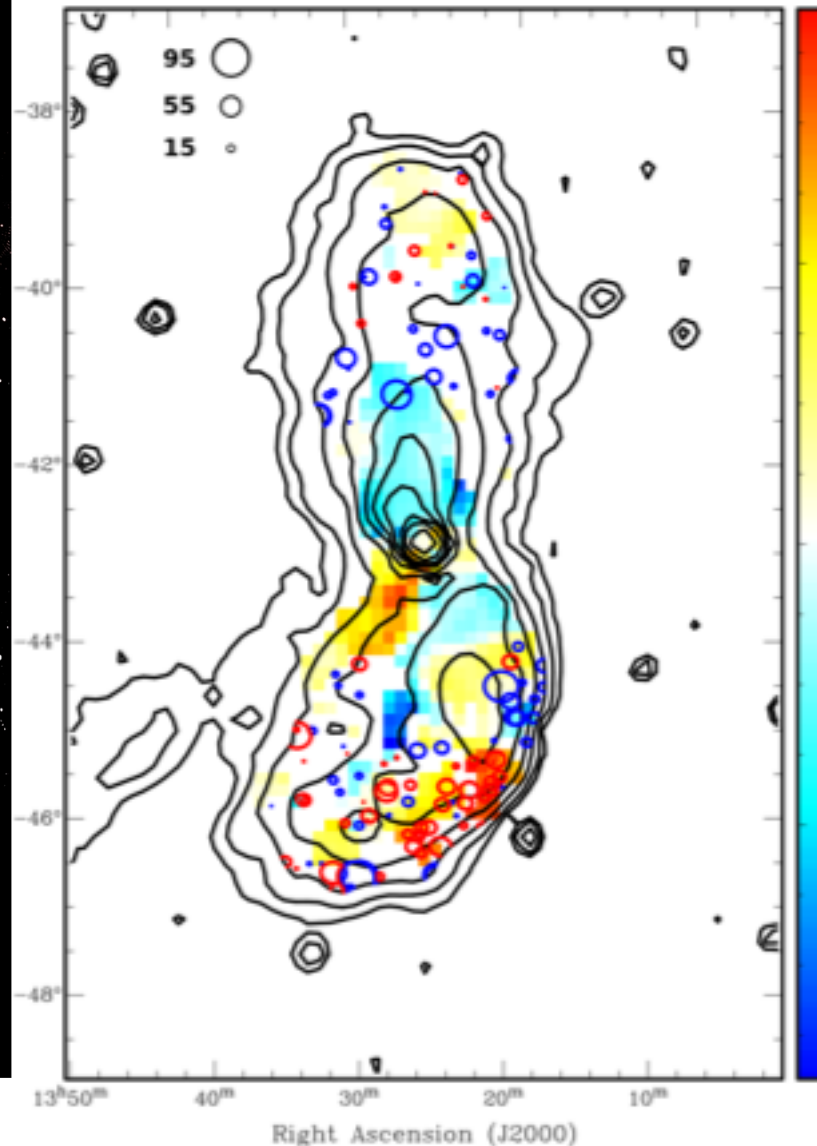


Z/Z_{\odot}	kT	Norm	$F_{0.5-2 keV}^{abs}$	red. χ^2/dof
(1)	(2)	(3)	(4)	(5)
Lobe 1				
1.0^f	$0.46^{+0.08}_{-0.11}$	$3.11^{+1.11}_{-0.53}$	5.84	1.20/444
0.3^f	$0.45^{+0.08}_{-0.10}$	$9.76^{+3.80}_{-1.88}$	6.12	1.20/444
0.1^f	$0.39^{+0.09}_{-0.07}$	$27.3^{+10.4}_{-7.2}$	6.72	1.20/444
Lobe 2				
1.0^f	$0.64^{+0.05}_{-0.05}$	$2.91^{+0.34}_{-0.35}$	5.83	1.13/515
0.3^f	$0.64^{+0.05}_{-0.05}$	$8.59^{+1.03}_{-1.03}$	6.20	1.13/515
0.1^f	$0.62^{+0.06}_{-0.06}$	$19.1^{+2.61}_{-2.49}$	6.72	1.13/515

$B \approx 1 \mu G$
 $kT \approx 0.5 keV$
 $n_g \approx 10^{-4} cm^{-3}$
 $M_g \approx 10^{10} M_{\odot}$
 $p_g \approx 8 \times 10^{-14} erg/cm^3 \approx (p_{e^+} + U_B)$
 $c_s \approx v_A \approx 3 \times 10^7 cm/s$

plasma- $\beta \approx 1$

Rotation Measure Studies

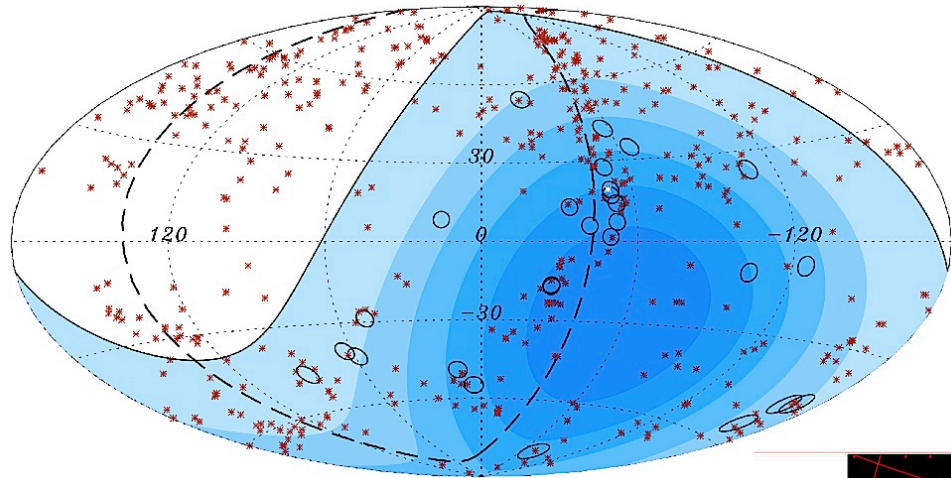


Feain et al. 2009, 2011,
O'Sullivan et al. 2013

Faraday rotation measure
(RM) study of the diffuse,
polarised, radio emission
from the giant lobes of
Centaurus A.

Foreground removed
through an ensemble of
background source RMs
located outside the giant
lobes. What is left is a
residual RM signal
associated with the giant
lobes. Most likely origin of
this residual RM is from
thermal material mixed
throughout the relativistic
lobe plasma.

UHECRs & Lobes?

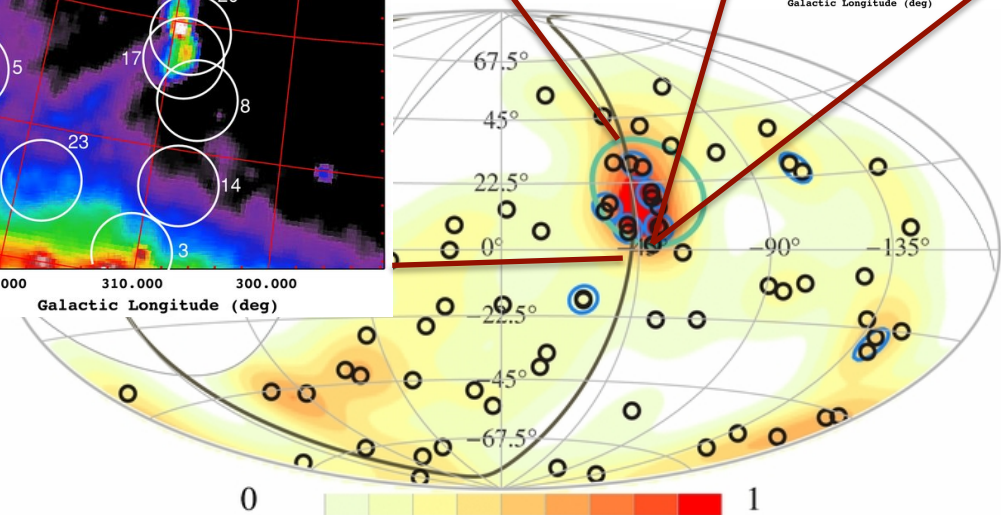
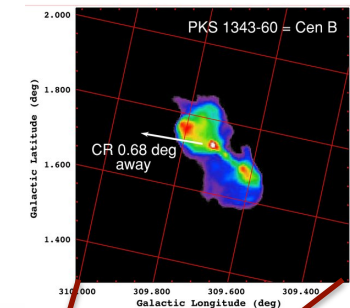
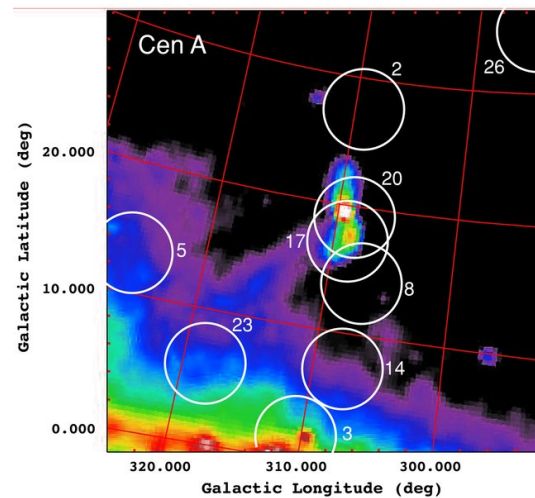


Abraham et al. 2007: Using data collected at the P. Auger Observatory during the first 3.7 years, a correlation between the arrival directions of cosmic rays with energy above 6×10^{19} eV and the positions of AGN within 75 Mpc was claimed.

An excess of UHECRs coincide with the position of Cen A (e.g., Moskalenko, LS et al. 2009, Yuksel et al. 2012, etc.)

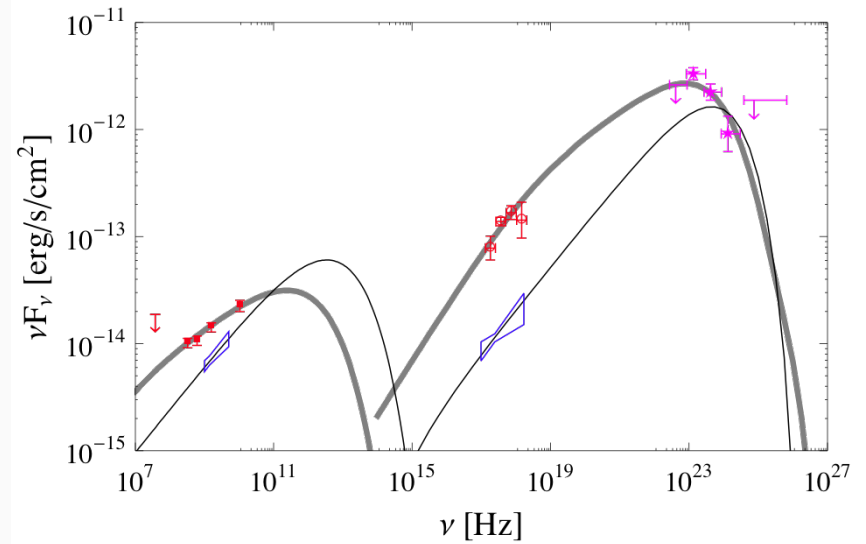
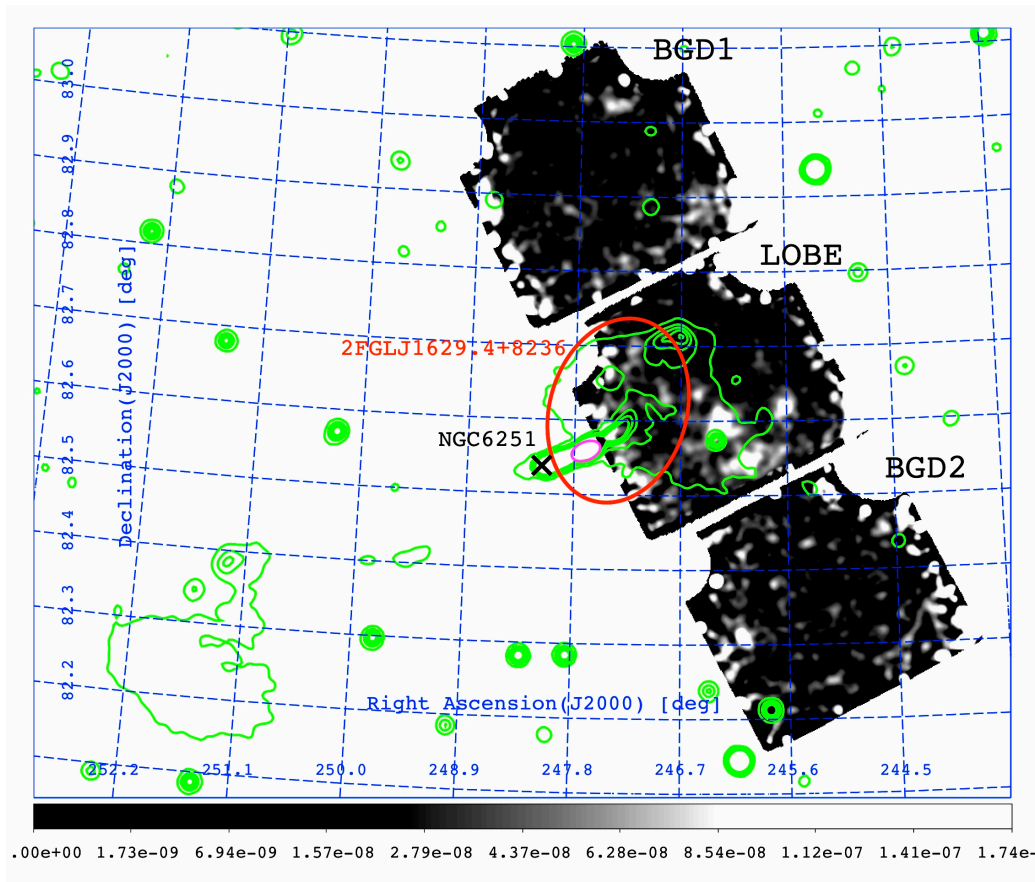
Stochastic acceleration of UHECRs in the Cen A giant halo requires rather large Alfvén speed (Hardcastle et al. 2009, O'Sullivan et al. 2009).

Our tentative detection of the thermal matter within the lobes challenges this idea.



Lobes in γ -rays: NGC 6251

Takeuchi et al. 2012

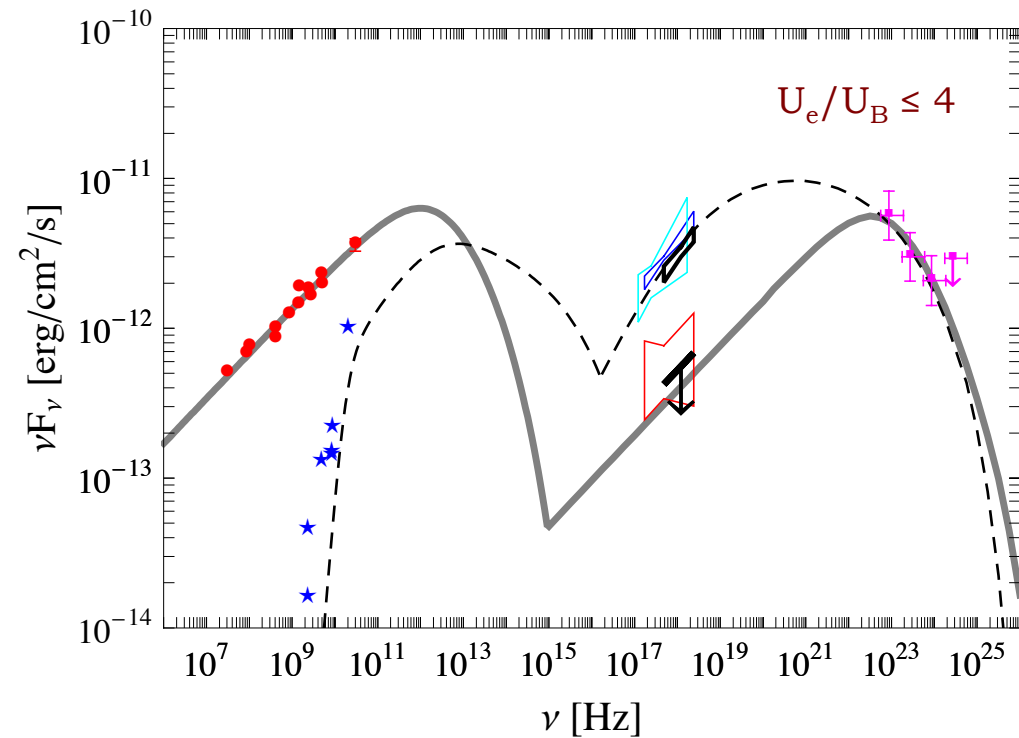
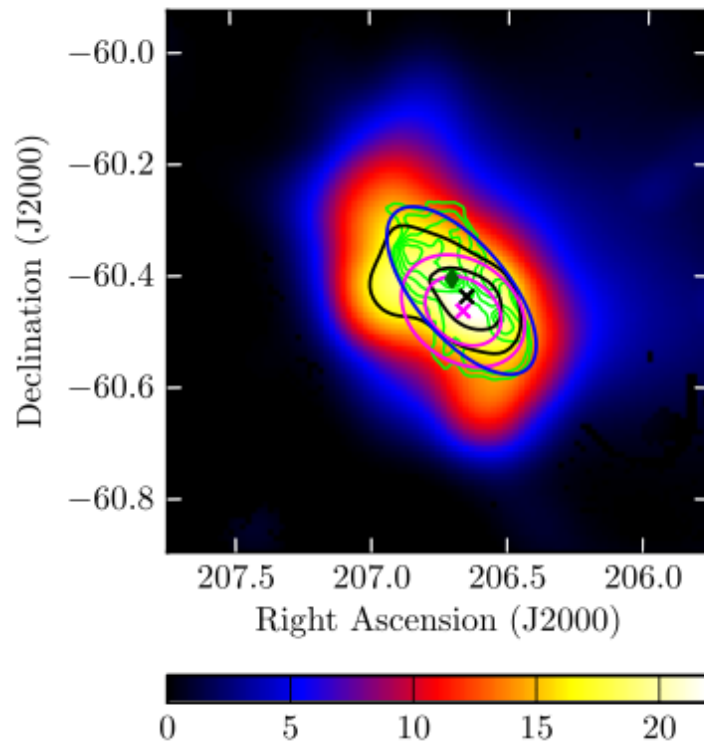


New Suzaku data and the re-analysis of the archival radio data implies that the giant lobe in NGC 6251 may be the source of the detected GeV photons.

$$U_e/U_B \sim 45$$

Lobes in γ -rays: Cen B

Katsuta et al. 2012

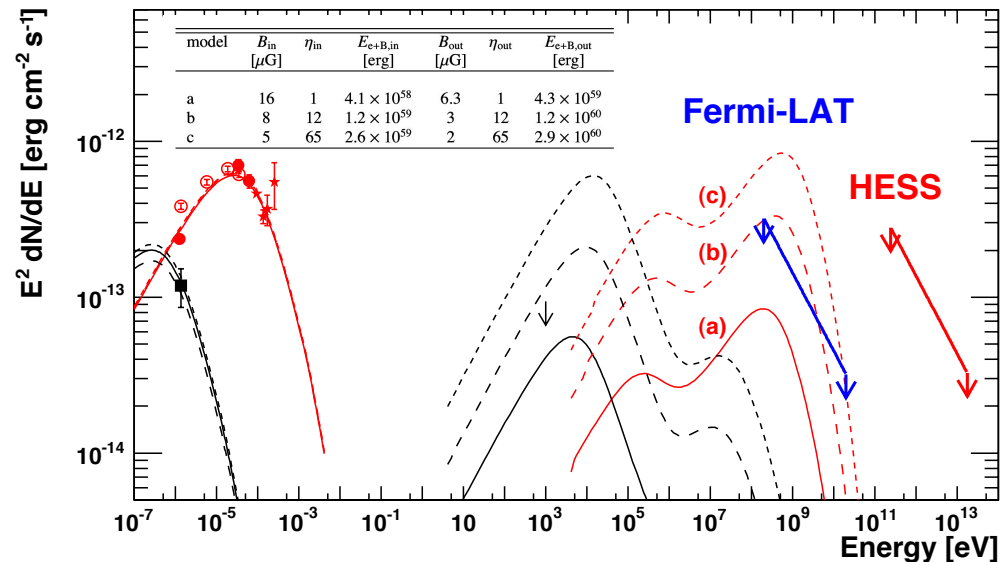
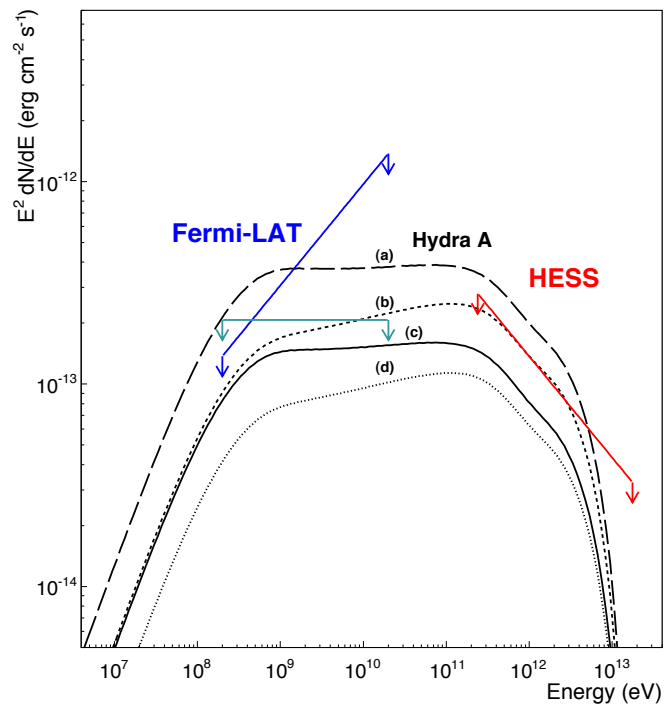
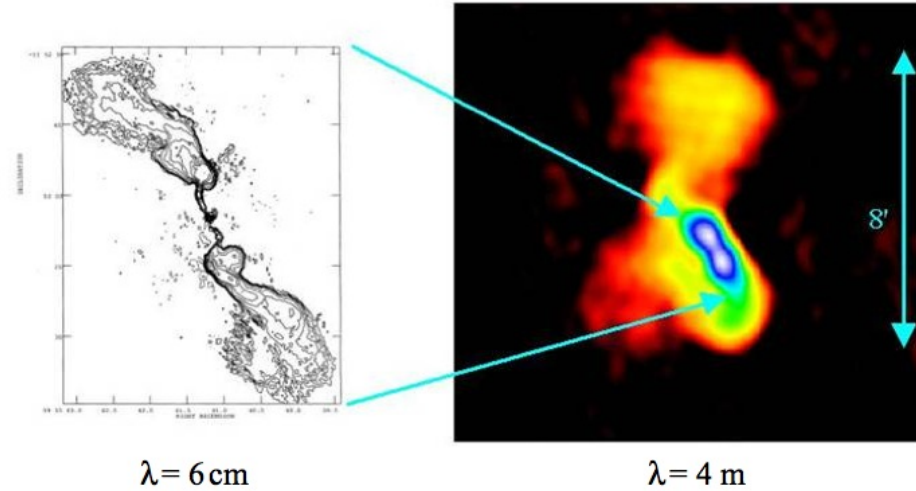


The broad-band modeling of the newly acquired Suzaku and LAT data for Cen B shows that the γ -ray flux of the source may in principle be produced within the extended lobes, if the diffuse non-thermal X-ray emission component is not significantly below the derived Suzaku upper limit. This would imply that efficient in situ acceleration of the ultrarelativistic particles is occurring and that the lobes are dominated by the pressure from the relativistic particles.

Lobes in γ -rays: Hydra A

- Abramowski et al. 2012, A&A
(CAs: Domainko, Hinton, Ohm & LS)

Gamma-ray and X-ray upper limits for the emission of the lobes in Hydra A exclude very weak magnetic fields and constrain the amount of relativistic proton support.



Circinus Galaxy

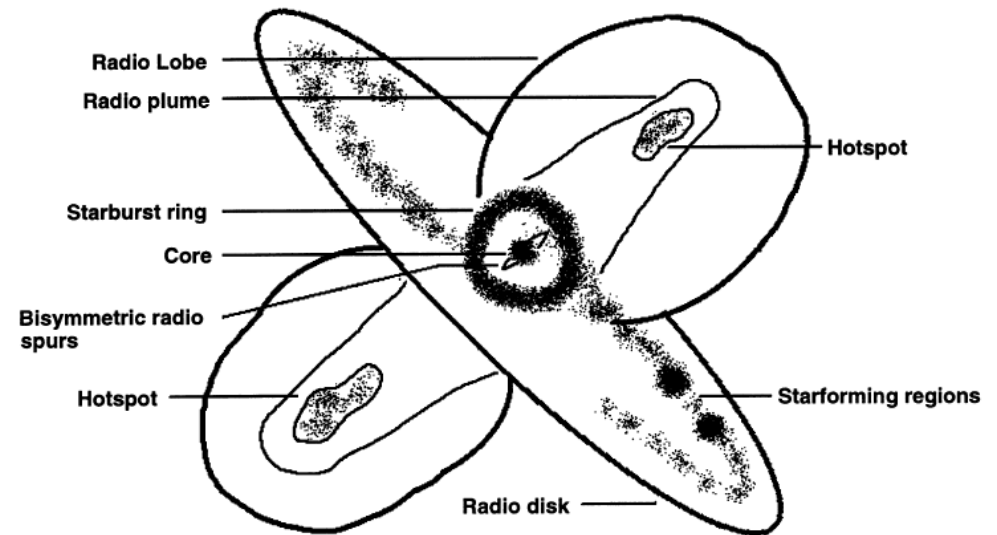
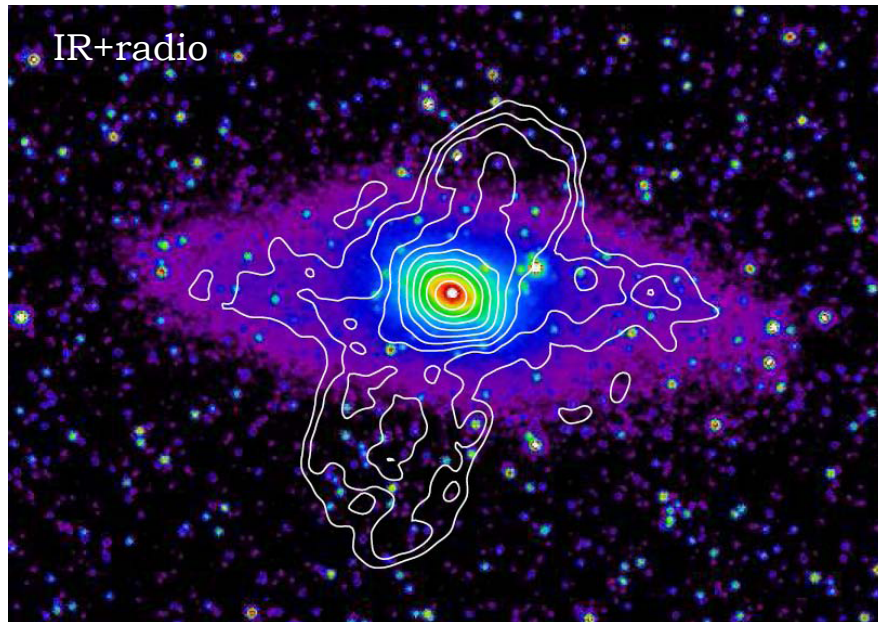
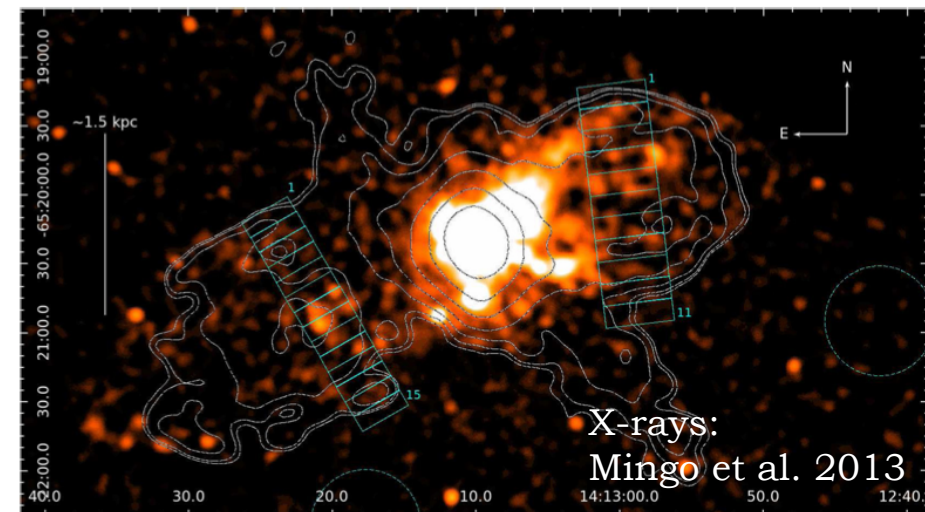
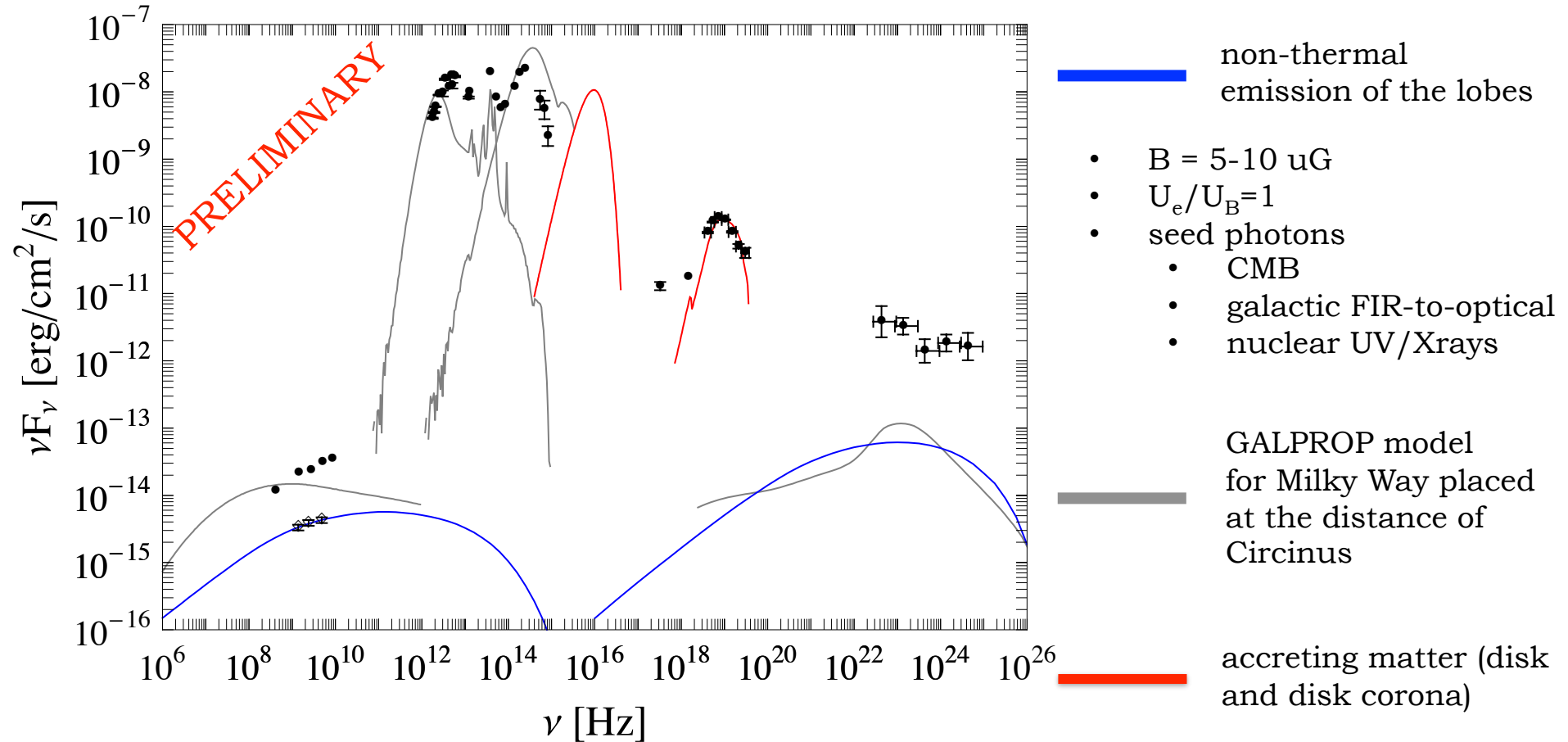


Figure 13. The proposed geometry for the radio continuum structures in Circinus. The figure is not to scale.

- Nearby active galaxy ($d = 4.2$ Mpc) with prominent starburst component;
- Active nucleus classified as heavily obscured (Compton-thick) and radio-quiet Seyfert.
- Large-scale radio lobes, detected also in X-rays with Chandra, believed to be due to the terminated jet activity (Elmouttie et al. 1998, Mingo et al. 2012); currently no evidence for a presence of nuclear jets.



Lobes?



Hayashida, LS, et al. 2013:
Circinus lobes can hardly account for the
observed GeV emission
(unless very far from the equipartition, or with
the dominant relativistic proton content).

Conclusions

- In situ electron acceleration within the extended lobes; acceleration of hadrons still an open question.
- A very complex magnetic structure with prominent large-scale filaments.
- A tentative detection of the thermal gas mixed with the non-thermal plasma.

Magnetic reconnection and turbulent acceleration processes continuously converting magnetic energy to the internal energy of the plasma particles, leading to possibly significant spatial and temporal variations in the plasma β parameter and pressure equilibrium condition

$$p_{th} \sim p_e \sim p_B.$$